CELL BIOLOGY

Metabolic responsiveness to training depends on insulin sensitivity and protein content of exosomes in insulin-resistant males

Maria Apostolopoulou[1,2,3†], Lucia Mastrototaro[2,3†], Sonja Hartwig[3,4], Dominik Pesta[2,3], Klaus Straßburger[3,5], Elisabetta de Filippo[2,3], Tomas Jelenik[2,3], Yanislava Karusheva[2,3], Sofiya Gancheva[1,2,3], Daniel Markgraf[2,3], Christian Herder[1,2,3], K. Sreekumaran Nair[6], Andreas S. Reichert[7], Stefan Lehr[3,4], Karsten Müssig[1,2,3], Hadi Al-Hasani[3,4], Julia Szendroedi[1,2,3,8], Michael Roden[1,2,3]*

High-intensity interval training (HIIT) improves cardiorespiratory fitness (VO_2max), but its impact on metabolism remains unclear. We hypothesized that 12-week HIIT increases insulin sensitivity in males with or without type 2 diabetes [T2D and NDM (nondiabetic humans)]. However, despite identically higher VO_2max, mainly insulin-resistant (IR) persons (T2D and IR NDM) showed distinct alterations of circulating small extracellular vesicles (SEVs) along with lower inhibitory metabolic (protein kinase Cε activity) or inflammatory (nuclear factor κB) signaling in muscle of T2D or IR NDM, respectively. This is related to the specific alterations in SEV proteome reflecting down-regulation of the phospholipase C pathway (T2D) and up-regulated antioxidant capacity (IR NDM). Thus, SEV cargo may contribute to modulating the individual metabolic responsiveness to exercise training in humans.

INTRODUCTION

Regular exercise training not only reduces cardiovascular risk but also helps to prevent and treat type 2 diabetes (T2D) (*1*, *2*). However, up to 20% of all T2D participants in exercise interventions fail to respond to physical training with improved glucose metabolism (*3*). Even first-degree relatives of persons with T2D do not necessarily increase their insulin sensitivity despite higher muscle adenosine 5′-triphosphate (ATP) synthase flux after 6 months of exercise training (*4*). Among other factors, exercise volume and intensity predict exercise responsiveness (*5*). High-intensity interval training (HIIT) represents a time-saving, highly efficient alternative to moderate training modalities and may exert superior beneficial effects (*6*), such as improved insulin sensitivity and mitochondrial function in elderly people (*7*). However, 9-day HIIT failed to enhance insulin sensitivity in insulin-resistant (IR) offspring of T2D despite increased mitochondrial function (*8*). It remains to be determined whether longer-term HIIT ameliorates mitochondrial changes and insulin sensitivity in IR people with or without T2D.

Metabolic effects of exercise result from intertissue communication via metabolites, hormones, myokines/exerkines, microRNA, or medium-sized extracellular vesicles (EVs) (*9*–*12*). Recent studies suggest that one exercise bout also leads to the release of exosome or small (30 to 200 nm) EVs (SEVs) by skeletal muscle in healthy volunteers (*13*–*15*). However, the role of SEV in IR humans and their impact on the metabolic response to a supervised exercise program per se, independent of diet or body weight changes, are not known. SEV can shuttle their functional content to target tissue to activate cellular signaling (*16*), but it is also unclear whether and, if so, which SEV cargo relates to changes in insulin sensitivity and underlying cellular pathways (*17*).

Thus, this study examined the effect of a supervised 12-week HIIT on metabolic features and SEV release in sedentary insulin-sensitive nondiabetic humans (IS NDM) and IR NDM glucose-tolerant—as defined by established papers (*18*)—as well as T2D individuals. We originally hypothesized that HIIT would uniformly ameliorate insulin sensitivity independently of glucose tolerance. Unexpectedly, metabolic responsiveness to HIIT, as defined by increased peripheral insulin sensitivity (*M* value), was more prevalent among the groups with insulin resistance before HIIT. This study therefore investigated next whether quantity and proteome of SEV help to differentiate between responders (T2D-R and IR-R from the T2D and IR NDM groups) and nonresponders (IS-NR from the IS NDM group). SEVs were isolated by size exclusion chromatography (SEC), allowing for subsequent downstream analysis (*19*), and characterized by nanoparticle tracking analysis (NTA) and mass spectrometry (MS) for protein identification and quantification. Last, we validated expression of selected SEV candidates in skeletal muscle biopsies. This study revealed that HIIT differently affects SEV concentration and their proteome depending on baseline insulin sensitivity in men, suggesting that SEV cargo modulates the individual metabolic responsiveness to exercising and may help to explain the variable success of physical training.

RESULTS

Participants' characteristics at baseline

Out of 49 persons, 20 T2D and 23 individuals without diabetes (NDM) completed the study (fig. S1). Cardiorespiratory fitness (VO_2max)

[1]Department of Endocrinology and Diabetology, Medical Faculty and University Hospital, Heinrich-Heine-University Düsseldorf, Düsseldorf, Germany. [2]Institute for Clinical Diabetology, German Diabetes Center, Leibniz Center for Diabetes Research at Heinrich-Heine-University Düsseldorf, Düsseldorf, Germany. [3]German Center for Diabetes Research, Partner Düsseldorf, München-Neuherberg, Germany. [4]Institute for Clinical Biochemistry and Pathobiochemistry German Diabetes Center, Leibniz Center for Diabetes Research at Heinrich-Heine-University Düsseldorf, Düsseldorf, Germany. [5]Institute for Biometrics and Epidemiology, German Diabetes Center, Leibniz Center for Diabetes Research at Heinrich-Heine-University Düsseldorf, Düsseldorf, Germany. [6]Division of Endocrinology, Diabetes and Nutrition, Mayo Clinic, Rochester, MN, USA. [7]Institute of Biochemistry and Molecular Biology I, Medical Faculty and University Hospital Düsseldorf, Heinrich-Heine-University Düsseldorf, Düsseldorf, Germany. [8]Department of Internal Medicine, Heidelberg University, Heidelberg, Germany.
*Corresponding author. Email: michael.roden@ddz.de
†These authors contributed equally to this work.

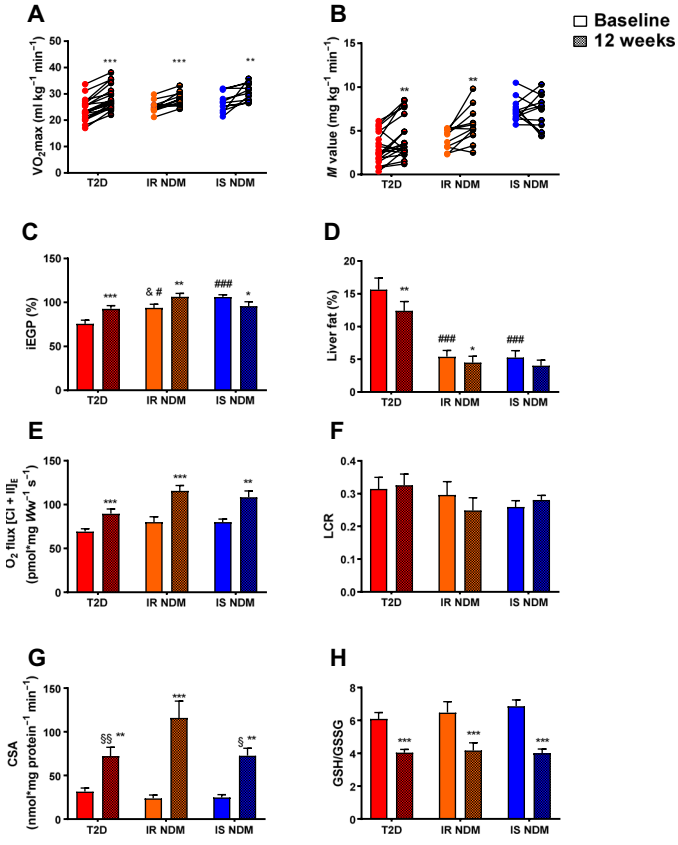

Fig. 1. HIIT induces metabolic changes and stimulates maximal skeletal muscle mitochondrial capacity in humans with (T2D) and without T2D (NDM). (**A**) Maximal oxygen uptake (VO_2max) (***$P = 0.00025$ for T2D, ***$P = 6.42 \times 10^{-5}$ for IR NDM, and **$P = 0.008$ for IS NDM), (**B**) peripheral insulin sensitivity (*M* value) (**$P = 0.003$ for T2D and **$P = 0.002$ for IR NDM), (**C**) hepatic insulin sensitivity [suppression of EGP (iEGP)] during high-insulin clamp (***$P = 0.0001$ for T2D, **$P = 0.007$ for IR NDM, and *$P = 0.02$ for IS NDM; #$P = 0.01$ T2D versus IR NDM, ###$P = 7.87 \times 10^{-7}$ T2D versus IS NDM; & $P = 0.04$ IR NDM versus IS NDM), (**D**) liver fat content (**$P = 0.003$ for T2D and *$P = 0.02$ for IR NDM; ###$P = 0.0005$ T2D versus IR NDM, ###$P = 7.17 \times 10^{-5}$ T2D versus IS NDM), (**E**) maximal uncoupled respiration (*Ww*, wet weight) (***$P = 3.73 \times 10^{-5}$ for T2D, ***$P = 0.0005$ for IR NDM, and **$P = 0.001$ for IS NDM), (**F**) leak control ratio (LCR), (**G**) citrate synthase activity (CSA) (**$P = 0.001$ for T2D, ***$P < 0.0001$ for IR NDM, and **$P = 0.004$ for IS NDM; §§$P = 0.004$ T2D versus IR NDM, §$P = 0.01$ IS NDM versus IR NDM at 12 weeks), and (**H**) reduced-to-oxidized glutathione (GSH/GSSG) ratio (***$P < 0.0001$ for T2D and IS NDM and ***$P = 0.0002$ for IR NDM) at baseline and after 12-week HIIT in persons with T2D, IR NDM, and IS NDM. Data are presented as means ± SEM.

was comparable between all groups (Fig. 1A). The high insulin clamp–derived *M* value reflects insulin-stimulated skeletal muscle glucose uptake (*20*). During both clamp periods, all three groups had comparable blood glucose and plasma insulin levels (Table 1). For separating IS from IR participants, we followed a previous publication that, using a similar insulin clamp protocol, defined *M* values of less than 5.5 mg kg^{-1} min^{-1} (under high insulin clamp conditions) as insulin resistance state in adult humans (*18*). This cutoff value allowed to identify 11 IR NDM and 12 IS NDM. The *M* values were lower in T2D and IR NDM than IS NDM ($P < 0.001$; Fig. 1B), even after the correction for insulin achieved during the clamp procedure. Insulin-mediated suppression of endogenous glucose production (iEGP), as the measure of hepatic insulin sensitivity, was lower ($P < 0.001$; Fig. 1C), whereas liver fat content was higher in T2D than in both NDM groups ($P < 0.001$; Fig. 1D). As expected, T2D also had higher hemoglobin A1c and lower high-density lipoprotein cholesterol than both NDM groups (Table 1). Compared to IS NDM, T2D had higher body mass index (BMI), partly due to higher visceral fat mass, whereas the greater BMI of IR NDM resulted from both higher subcutaneous and visceral fat mass (Table 1). Fasting plasma glucose was higher in the T2D group compared to the NDM groups, whereas fasting plasma insulin was only different between T2D and IS NDM (Table 1).

HIIT uniformly improves whole-body oxidative and skeletal muscle mitochondrial capacity

After 12 weeks of HIIT, all participants uniformly increased their VO_2max (Fig. 1A) despite unchanged body weight and whole-body fat content (Table 1). O_2 fluxes upon adenosine diphosphate (ADP) and substrates, assessed ex vivo in permeabilized skeletal muscle fibers, were similar between groups and after HIIT, except for O_2 fluxes through complex I (CI_P) and CI + II_P, which tended to be higher after HIIT in IS NDM (fig. S2A). On the other hand, maximal uncoupled respiration (CI + II_E) tended to be lower in T2D than in IS NDM at baseline ($P = 0.06$) but rose by 28 to 45% in all groups after HIIT (Fig. 1E). The leak control ratio (LCR), reflecting increased proton leak across the mitochondrial membrane, remained unchanged (Fig. 1F), whereas muscle citrate synthase activity (CSA), as a surrogate marker of mitochondrial content (*21*), at least doubled after HIIT in all groups with the greatest rise in IR NDM (Fig. 1G). Moreover, HIIT decreased the concentration of reduced glutathione (GSH) but not oxidized glutathione (GSSG) and consequently the ratio of reduced to oxidized glutathione (GSH/GSSG), a sensitive biomarker of tissue redox state (*22*), in all participants (Fig. 1H and fig. S3), but it did not affect the hydrogen peroxide (H_2O_2) emission in any group (fig. S2B). However, after normalization to CSA, HIIT also diminished the rate of H_2O_2 emission by mitochondria respiring on pyruvate/malate/glutamate (CI) in IR NDM and on succinate and rotenone (CII) in IS NDM (fig. S2C).

Mainly IR persons (T2D and IR NDM) exhibit increased peripheral insulin sensitivity upon HIIT

Despite consistent gain in whole-body and skeletal muscle oxidative capacity, the metabolic response to HIIT substantially varied, as shown by the percent changes in the *M* values (fig. S4A). The present study defined an increase in *M* value following 12 weeks of exercising (ΔM value > 0) to separate (metabolic) responders from nonresponders to HIIT. Table S1 depicts the anthropometric and metabolic parameters of responders and nonresponders within each group. Logistic regression analysis showed an approximately doubled probability of the responder status among T2D (16 of 20; 80%) and IR NDM (9 of 11; 82%) as compared to IS NDM (5 of 12; 42%) ($\beta = 1.94$, $P = 0.02$ and $\beta = -2.2$, $P = 0.03$, respectively). Likewise, only the IR groups, T2D and IR NDM, ameliorated their mean peripheral (Fig. 1B) and hepatic insulin sensitivity (Fig. 1C) as well as liver fat content (Fig. 1D). However, the responders among the IS NDM (IS-R) also increased their peripheral insulin sensitivity (fig. S4B). Only in T2D, HIIT also reduced visceral fat content, serum free fatty acids (FFA), and triglycerides (TG) and showed a trend toward decreased serum glutamic-pyruvic transaminase (SGPT; $P = 0.06$) (Table 1).

Table 1. Anthropometric and metabolic parameters at baseline and after 12 weeks of HIIT in patients with T2D, IR controls (IR NDM), and IS controls (IS NDM). BMI, body mass index; HbA1c, hemoglobin A1c; SGPT, serum glutamic-pyruvic transaminase; LDL, low-density lipoprotein; HDL, high-density lipoprotein; Δfasting insulin, difference between fasting insulin at 12 weeks versus baseline; Δinsulin clamp, difference between insulin during high insulin clamp and insulin before the clamp. Data are shown as means ± SEM or median (q1, q3). &$P < 0.05$, &&$P < 0.01$, and &&&$P < 0.001$ T2D versus IS NDM; §$P < 0.05$, §§$P < 0.01$, and §§§$P < 0.001$ T2D versus IR NDM; #$P < 0.05$ and ##$P < 0.01$ IS NDM versus IR NDM; *$P < 0.05$, **$P < 0.001$, and ***$P < 0.00001$ 12 weeks versus baseline.

Parameter	T2D ($n = 20$)		IR NDM ($n = 11$)		IS NDM ($n = 12$)	
	Baseline	12 weeks	Baseline	12 weeks	Baseline	12 weeks
Age (years)	57 ± 1		56 ± 1		58 ± 1	
BMI (kg/m^2)	31.2 ± 0.6$^{\&}$	30.8 ± 0.6	32.2 ± 0.7	32.1 ± 0.7	29.3 ± 0.6$^{\#\#}$	29.1 ± 0.4
Whole-body fat (kg)	26.5 ± 1.1	26.5 ± 1.4	29.6 ± 1.9	29.1 ± 2.1	23.9 ± 1.4$^{\#}$	23.1 ± 1.4
Visceral fat (kg)	5.9 ± 0.4$^{\&\&}$	5.5 ± 0.4*	5.4 ± 0.4	5.4 ± 0.4	4.4 ± 0.2$^{\#}$	4.1 ± 0.2
Subcutaneous fat (kg)	20.6 ± 1.1	20.9 ± 1.3	24.2 ± 1.8	23.7 ± 1.9	19.5 ± 1.4$^{\#}$	18.9 ± 1.3
HbA1c (%)	7.2 ± 0.2$^{\&\&\&\S\S\S}$	6.9 ± 0.2	5.4 ± 0.1	5.3 ± 0.1	5.4 ± 0.1	5.5 ± 0.1
SGPT (U/liter)	41 (29, 62)$^{\&\&}$	33 (25, 61)	29 (20, 37)	27 (19, 32)	24 (21, 29)	24 (20, 29)
Free fatty acids (μM)	523 ± 38	369 ± 26***	504 ± 59	463 ± 44	415 ± 50	411 ± 59
Triglycerides (mg/dl)	152 (125, 231)	119 (90, 173)**	131 (102, 163)	132 (100, 143)	121 (82, 149)	128 (81, 160)
LDL-cholesterol (mg/dl)	132 ± 8§	128 ± 7	158 ± 9	153 ± 12	149 ± 7	133 ± 9
HDL-cholesterol (mg/dl)	46 ± 3$^{\S\&}$	51 ± 3*	55 ± 3	56 ± 3	55 ± 4	50 ± 4*
Fasting blood glucose (mg/dl)	152 ± 42$^{\S\S\&\&}$	137 ± 31*	85 ± 5	84 ± 7	86 ± 4	85 ± 3
Glucose (low clamp) (mg/dl)	91 ± 1	90 ± 1	89 ± 1	88 ± 2	90 ± 1	91 ± 2
Glucose (high clamp) (mg/dl)	89 ± 1	90 ± 1	90 ± 2	89 ± 1	89 ± 2	90 ± 1
Fasting insulin (μU/ml)	14 (8, 25)$^{\&}$	16 (11, 24)	10 (8, 13)	9 (6, 14)	8 (6, 10)	8 (6, 11)
ΔFasting insulin (μU/ml)		0.5 (−0.7, 3.8)		1.6 (0.4, 4.4)		−0.9 (−3.4, 0.9)
Insulin (low clamp) (μU/ml)	25 (23, 28)	25 (23, 33)	12 (17, 31)	25 (19, 29)	26 (21, 34)	26 (21, 29)
Insulin (high clamp) (μU/ml)	60 (45, 64)	59 (47, 67)	50 (34, 71)	52 (47, 62)	60 (45, 64)	59 (48, 64)
M value per high clamp insulin (mg kg^{-1} min^{-1})/(μU/ml)	0.04 (0.03, 0.07)$^{\&\&}$	0.06 (0.04, 0.13)*	0.08 (0.06, 0.10)$^{\#\#}$	0.08 (0.07, 0.16)*	0.12 (0.09, 0.17)	0.12 (0.08, 0.15)
M value per Δinsulin clamp (mg kg^{-1} min^{-1})/(μU/ml)	0.09 (0.05, 0.12)$^{\&\&}$	0.10 (0.06, 0.15)*	0.10 (0.07, 0.12)$^{\#}$	0.10 (0.09, 0.18)	0.13 (0.12, 0.20)	0.14 (0.10, 0.17)

HIIT differently affects myocellular pathways of insulin sensitivity in the IR responders (T2D-R and IR-R)

To further examine the heterogeneous responses of the insulin sensitivity (*M* value) within the groups, we used skeletal muscle biopsies from the subgroups, which substantially differed at baseline and after HIIT, i.e., IR responders (T2D-R, $N = 16$; IR-R, $N = 9$) and IS nonresponders (IS-NR, $N = 7$) (Fig. 2A). For better data interpretation, we conducted the molecular analysis also in the IR nonresponders (T2D-NR and IR-NR) and in the IS responders (IS-R) (fig. S4, B to J). We primarily addressed key mechanisms known to underlie human myocellular insulin resistance, such as abnormal mitochondrial function and inhibitory lipid signaling via activation of the diacylglycerol/novel protein kinase C isoform (DAG/nPKC) pathway and/or inhibitory inflammatory pathways (*23*–*25*). Similar to the whole groups, HIIT elevated mitochondrial function (Fig. 2B) and decreased the GSH/GSSG ratio in all subgroups (Fig. 2C). Activation of the nPKCε and θ isoforms was assessed from translocation of the respective proteins to the myocellular membrane (fig. S5A). PKCε activity negatively associated with *M* value (log-transformed; $\beta = -0.55$; $P = 0.002$) at baseline, but not after HIIT. At baseline, PKCε activity was doubled in T2D-R compared to IR-R and IS-NR (Fig. 2D). After HIIT, T2D-R exhibited 50 and 40% decreases in PKCε and θ activities, respectively (Fig. 2, D and E). Additional measurement of the nPKC activities in the whole groups of T2D, IR NDM, and IS NDM showed an identical pattern (fig. S5, B and C), suggesting that the nPKC pathway could be involved in improvement in insulin resistance by HIIT at least in overt T2D.

Inflammatory pathways, specifically nuclear factor κ light chain enhancer of activated B cells (NF-κB), not only relate to insulin resistance and oxidative stress but may also be down-regulated by chronic exercising (*26*, *27*). Thus, we also analyzed muscle NF-κB protein levels in all groups, which did not differ between responders and nonresponders at baseline but were reduced by 24% after HIIT exclusively in IR-R (Fig. 2F). This exercise effect was confirmed in the whole groups of T2D, IR NDM, and IS NDM, although baseline NF-κB levels were 40% higher in T2D compared to IS NDM (fig. S5D). However, circulating pro- and anti-inflammatory cytokines interleukin-1β (IL-1β), IL-6, IL-15, and IL-1ra and tumor necrosis factor–α (TNFα) were not significantly different between groups and after HIIT. These data suggest that the metabolic response to HIIT could be associated to the decrease of nPKC activity in responders with diabetes (T2D-R) and to the reduction of activation of NF-κB–dependent pathways in responders without diabetes (IR-R).

HIIT induces an increase in circulating SEV in the IR responders (T2D-R and IR-R)

To clarify the role of SEV in exercise response, we measured the effect of HIIT on SEV release in representative subgroups of T2D-R ($N = 8$), IR-R ($N = 8$), and IS-NR ($N = 6$). These subgroups showed overall similar changes as the whole cohort, i.e., increased VO_2max and mitochondrial respiration in all, but increased peripheral and hepatic insulin sensitivity only in T2D-R and IR-R (fig. S6, A to D). Also, only T2D-R showed reduced PKCε activation (fig. S6E), whereas only IR-R had lower NF-κB levels (fig. S6F).

We measured the size and the number of circulating SEV in serum of responders and nonresponders, collected at baseline and 72 hours after the last bout of the 12-week HIIT. We characterized SEV preparations by NTA, transmission electron microscopy (TEM), and immunoblotting for typical EV markers (CD9, CD63, and HSP70), major components of non-EV coisolated structures (albumin), and proteins associated with other intracellular compartment than plasma membrane (calnexin) (Fig. 3, A to C, and fig. S7A) (*13*). The mean diameter of the isolated SEV was about 100 nm with a peak at about 80 nm, as shown by NTA, and comparable between groups before and after HIIT (Fig. 3D). The estimated SEV concentration (number of circulating SEV per protein) was higher in IS-NR compared to T2D-R and numerically higher than in IR-R at baseline (Fig. 3E). After HIIT, the SEV concentration rose only in the IR groups, T2D-R and IR-R (Fig. 3F), with an increase of 52% [expressed as $\log_2$ fold change (FC)] for both groups (fig. S7B).

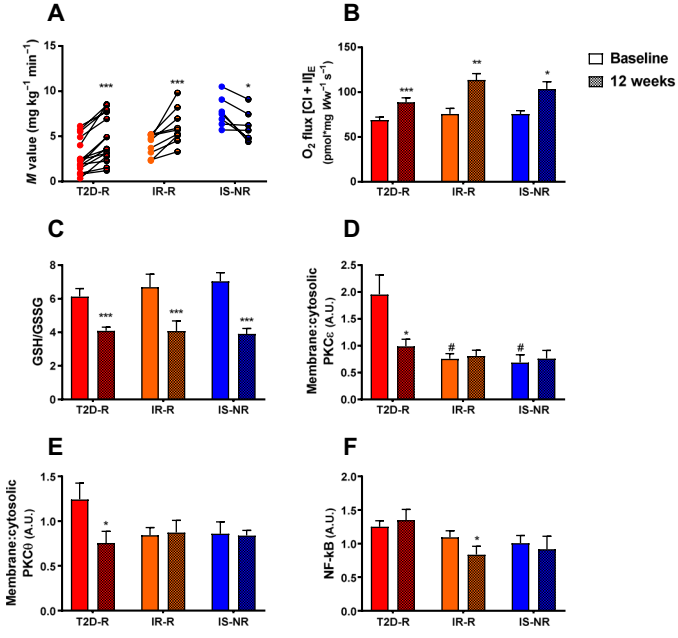

Fig. 2. HIIT differently affects myocellular pathways of insulin sensitivity in the IR responders (T2D-R and IR-R). (**A**) *M* value (***$P = 3.88 \times 10^{-5}$ for T2D-R, ***$P = 1.79 \times 10^{-5}$ for IR-R, and *$P = 0.02$ for IS-NR), (**B**) maximal uncoupled respiration (***$P = 0.0002$ for T2D-R, **$P = 0.002$ for IR-R, and *$P = 0.02$ for IS-NR), (**C**) GSH/GSSG ratio (***$P < 0.0001$ for T2D-R, ***$P = 0.0009$ for IR-R, and ***$P = 0.0002$ for IS-NR), (**D**) protein kinase Cε (PKCε) (*$P = 0.02$ for T2D-R; #$P = 0.02$ T2D-R versus IR-R, #$P = 0.04$ T2D-R versus IS-NR), (**E**) PKCθ (*$P = 0.03$ for T2D-R), and (**F**) NF-κB (*$P = 0.01$ for IR-R) Western blot analysis in the subgroups T2D-R ($N = 16$), IR-R ($N = 9$), and IS-NR ($N = 7$) at baseline and after 12-week HIIT. Data are expressed as means ± SEM. A.U., arbitrary units.

As HIIT increased the number of circulating SEV only in the IR responders, we hypothesized that SEV and their content could contribute to the different cellular metabolic adaptations to this mode of chronic exercise training. We therefore characterized the proteome of the SEV isolated from T2D-R ($N = 5$), IR-R ($N = 5$), and IS-NR ($N = 5$) individuals at baseline and after HIIT and identified a total of 1707 proteins including the 24 exosomal-enriched proteins as well as serum proteins, such as albumin, apolipoproteins, and immunoglobulins, which represent contaminants copurified with all isolation methods (table S2) (*28*). We found that 809 proteins of serum SEV overlapped with proteins identified in SEV isolated from three human cell lines (skeletal muscle cells, smooth muscle cells, and adipocytes; table S2) and therefore bona fide represented SEV proteins.

Furthermore, 1589 of the identified proteins (98%) overlapped with the human EV-associated proteins previously identified in the Vesiclepedia database (13,550 unique protein entries), whereas 39 were newly found as SEV-carried proteins (Fig. 4A and table S3). Among the total SEV-associated proteins, we then selected the candidates with low variability ($q < 0.05$) and high degree of regulation (absolute log FC between groups or baseline versus HIIT > 0.5), and we found that the proteomic profile differed between groups at baseline (see Supplementary Text) and after HIIT.

HIIT affects the proteomic profile of SEV

Quantitative proteomic analysis revealed that HIIT regulates the expression of 262 SEV proteins ($n = 122$ in T2D-R, $n = 130$ in IR-R, and $n = 89$ in IS-NR), of which 102 were down-regulated and 160 were up-regulated (Fig. 4B and table S4). Among the regulated SEV proteins, we identified proteins typically associated with exosomes (*29*), such as biogenesis markers (ALIX), signaling proteins (guanosine triphosphatase and Ras-related protein), proteins associated with membrane trafficking and fusion (Rab proteins and annexins), lipid rafts (flotillin), cytoskeleton components (moesin and tubulin), and cell adhesion molecules (integrins). Moreover, the cellular component (CC) enrichment analysis of regulated SEV proteins confirmed a significant enrichment of proteins associated with extracellular exosomes (Fig. 4C). Notably, 13 of the 262 SEV proteins, differentially expressed after HIIT, were shared between all groups (Fig. 4D and table S4), including antithrombin III, kininogen I, histidine-rich glycoprotein, and α1-antitrypsin, which relate to inflammatory and immune responses (*30*). Moreover, 29 SEV proteins were up- or down-regulated after HIIT exclusively in responders but not in IS-NR (Fig. 4D and table S4). Among these proteins, fibrinogen α, β, and γ chains (FGA, FGB, and FGG, respectively) were similarly up-regulated in SEV isolated from T2D-R and IR-R after HIIT. These acute-phase proteins are not only associated with insulin resistance and acutely increased by insulin in T2D (*31*) but have also been described as myokine candidates carried by EV and released from the exercising limb after recovery (*15*), suggesting that exercise might activate insulin-sensitizing pathways. Notably, these proteins were different between groups at baseline, with the lowest levels in SEV derived from IS-NR and the highest levels in SEV of T2D-R, suggesting a role for FGA, FGB, and FGG for the observed improvements of insulin resistance.

Proteomic profiling of SEV suggests a new mode of myokine release for the metabolic adaptation to exercising

Since the 12-week HIIT triggered the release of SEV, we assumed that SEV might represent an alternative to the release of biologically

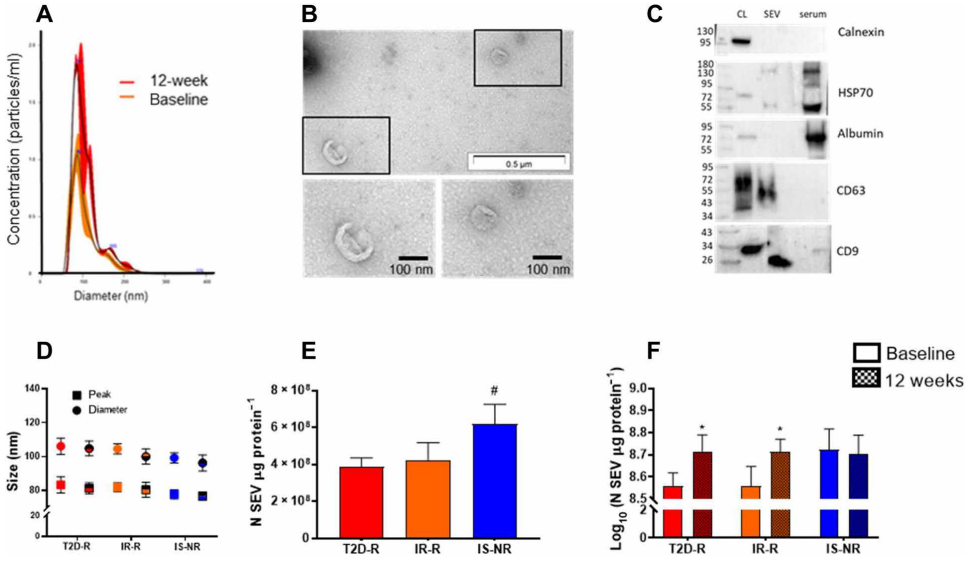

Fig. 3. HIIT intervention increases the release of circulating SEVs in humans with T2D-R and IR-R but not in IS-NR to exercising. (**A**) Representative distribution profiles of SEV isolated from serum of a patient with T2D at baseline (red plot) and after 12-week HIIT (orange plot); (**B**) morphology of serum SEV imaged using TEM (scale bars, 100 nm); (**C**) Western blot analysis of proteins extracted from cell lysate (HepG2), SEV, and the original serum before SEC (diluted 1:15); (**D**) plots of peak and diameter sizes of SEV isolated from T2D-R ($N = 8$), IR-R ($N = 8$), and IS-NR ($N = 6$) at baseline and after 12-wk HIIT; (**E**) number of circulating SEV at baseline (#$P = 0.04$ T2D-R versus IS-NR); and (**F**) number of circulating SEV $\log_{10}$-transformed at baseline and after 12-week HIIT (*$P = 0.01$ for T2D-R and *$P = 0.02$ for IR-R) in the pilot group including T2D-R ($N = 8$), IR-R ($N = 8$), and IS-NR ($N = 6$) humans. Data are expressed as means ± SEM.

active proteins by classical secretory pathway. We found that only 34% (89 of 262) of the proteins differentially expressed after HIIT had a predicted secretory signal peptide (SP), and only 12% (32 of 262) were predicted to follow a nonclassical secretion pathway, based on the bioinformatic tools SignalP and SecretomeP (Fig. 4E and table S4). These findings suggest that a large number of proteins can enter the circulation within SEV and that SEV can thereby contribute to interorgan communication affecting cellular metabolism. To examine whether HIIT-induced increase in circulating SEV—at least partially—originated from skeletal muscle, we performed another quantitative proteomic analysis of SEV released from primary human skeletal muscle cells (hSkMCs) using electrical pulse stimulation (EPS) to simulate the in vivo exercise intervention under in vitro conditions (Fig. 4F and table S5). Forty-four SEV proteins regulated after HIIT were also present in SEV collected from the media of EPS-trained hSkMC, suggesting that these SEV proteins could represent previously undiscovered myokines. Some of the SEV proteins regulated, both after HIIT in vivo and after EPS in vitro, are involved in signal transduction (GO:0007165; Ras-related proteins Rap1b and Rap2b), in oxidation-reduction processes (GO:0055114; aldehyde dehydrogenase family 16 member A1), and in cellular response to oxidative stress (GO:0034599; protein/nucleic acid deglycase DJ1 and peroxiredoxin-2).

HIIT enriches SEV with proteins related to insulin sensitivity in T2D-R and inflammation and oxidative metabolism in IR-R

We subsequently subjected the 262 SEV proteins differentially regulated by HIIT to Gene Ontology (GO) analysis of biological processes (BP) and molecular function (MF) and to Ingenuity Pathway Analysis (IPA), as described in Supplementary Text. To assess whether SEV protein cargo is responsible for the different metabolic adaptations induced by exercise in responders and nonresponders, we performed a functional analysis of the exercise-regulated SEV proteins in each group (T2D-R, IR-R, and IS-NR) and found different enriched GO terms and pathways (table S6).

In T2D-R, functional analysis revealed a significant enrichment of proteins linked to glycolytic process and predicted the inhibition of glycolysis (z score, −2), phospholipase C (PLC) (z score, −2), mitogen-activated protein kinase (ERK/MAPK) (z score, −2.236), and protein kinase A (PKA) signaling (z score, −2.249), based on the changes of the expression levels of SEV proteins associated to these pathways after HIIT (glycolysis: ENO1, PGK1, PKM, and TPI1; ERK/MAPK: HSPB1, PRKACB, PRKAR1A, RAB1B, and PRKCB; PLC: BTK, GNAQ, PRKCB, and RAB1B; PKA: GNAQ, MYLK, PRKACB, PKACB, PRKAR1A, PRKCB, and RAB1B) (Fig. 5A). In line with the pathway analysis, IPA identified MAPK1 and IL-15 as upstream molecules inhibited after HIIT (z score, −2.000 for both).

In SEV isolated from IR-R, we found an overrepresentation of the noncanonical NF-κB– and TNF-mediated pathways with up-regulation of the 20*S* core proteasome complex (PSMA1, PSMA3, PSMA5, PSMA6, PSMA7, PSMB1, PSMB5, and PSMB8) (*32*, *33*) as well as the process "cellular response to oxidative stress" with an up-regulation of proteins belonging to the cellular antioxidant system (CAT, CCS, G6PD, NME2, PRDX1, PRDX2, and SOD2) (Fig. 5B). In line, IPA predicted the overrepresentation of pentose phosphate pathway, with an up-regulation of glucose-6-phosphate dehydrogenase (G6PD), the rate-controlling enzyme of this pathway (*34*), as well as the activation of the upstream molecule NFE2L2 (z score, 2.607) and the NRF2-mediated oxidative stress response (z score, 2), since the downstream targets of NRF2 (CAT, PRDX1, PRKCA, RAB1B, SOD2, and AKR7A2) were up-regulated after HIIT. IPA also revealed IL-15 as an activated upstream regulator (z score, 2.224), probably stimulated by the antioxidant system (*35*). Last, in the IR groups, we found an enrichment of proteins associated to "response to calcium ion,"

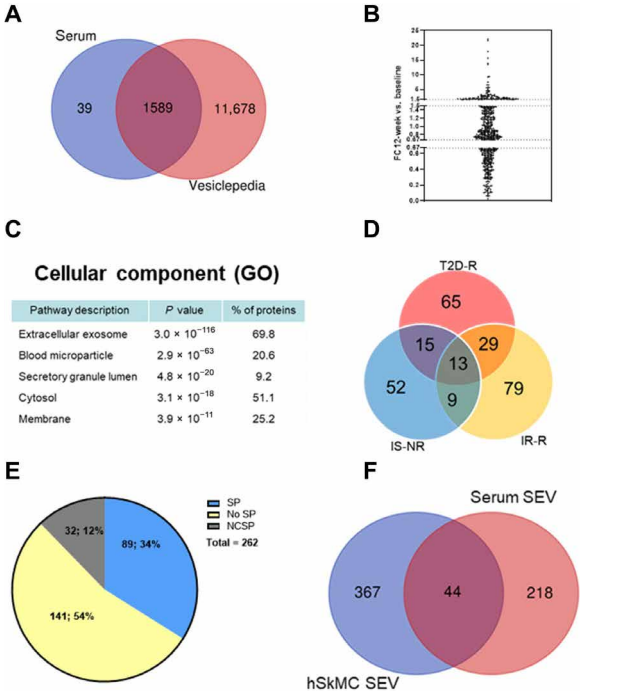

Fig. 4. Characteristics of SEV proteins differentially regulated after the 12-week HIIT. (**A**) Venn diagram showing the overlap of the proteins identified in serum SEV with the human protein entries in the EV database Vesiclepedia. Gene products were matched in FunRich. (**B**) Volcano plot depicting the FCs in proteins isolated from circulating SEV comparing 12-week HIIT versus baseline: Only proteins with an FC of <0.67 or >1.5 (absolute log FC > 0.5) were included for further analysis. (**C**) GO-CC analysis for the 262 SEV proteins regulated after the 12-week HIIT with *P* value and percentage of proteins. (**D**) Venn diagram showing the overlap of proteins regulated after the 12-week HIIT among the three groups. (**E**) Amino acid sequences of the SEV proteins regulated during exercise (262 entries) were analyzed to predict the presence of a secretory signal peptide (SP). (**F**) Venn diagram showing the overlap of proteins regulated after 12-week HIIT in circulating SEV and after EPS in hSkMC-derived SEV in vitro.

extending the concept of the involvement of Ca^{2+} in EV release (Fig. 5, A and B) (*36*). In IS-NR, we found a "lipid metabolism and transport" signature (Fig. 5C), and IPA revealed "autophagy of cells" as a cellular function associated only with SEV derived from IS-NR after the 12-week HIIT [Benjamini-Hochberg (B-H) $P < 0.05$; *z* score, 1.432].

We also conducted the functional analysis of the SEV proteins regulated by HIIT excluding the most abundant serum proteins in each group (immunoglobulin, albumin, and apolipoprotein). We found the same pathways for T2D-R and IR-R, whereas in IS-NR, we confirmed only the autophagy of cells.

Together, these results from associative studies suggest that HIIT could (i) down-regulate SEV proteins involved in the MAPK, PLC, and PKA signaling, which may contribute to stimulating the downstream insulin signaling pathway in T2D-R and (ii) enhance the antioxidant system in the SEV released by IR-R, which eventually leads to improved peripheral insulin sensitivity, while it (iii) does not seem to affect any SEV proteins known to be involved in insulin signaling in IS-NR. Nevertheless, the role of SEV for insulin signaling and responses to lifestyle modification in vivo will require further investigation.

SEV-cargoed proteins released after HIIT may directly affect cellular pathways in skeletal muscle

Last, for investigating whether the specific SEV proteins also affect molecular pathways in skeletal muscle, we measured selected candidates related to insulin signaling for validation in muscle biopsies of T2D-R, IR-R, and IS-NR individuals (fig. S8). Activating Thr^{172} phosphorylation of adenosine monophosphate–activated protein kinase (AMPK) was higher in T2D-R than in IR-R at baseline and after HIIT (Fig. 6A). Inhibitory Ser^{307} phosphorylation of insulin receptor substrate 1 (IRS1) was numerically lower in IR-R after HIIT ($P = 0.13$), whereas Ser^{1101} phosphorylation of IRS1 was not different between the groups (Fig. 6, B and C). In addition, NRF2 and its downstream target NADPH (reduced form of nicotinamide adenine dinucleotide phosphate) quinone dehydrogenase 1 (NQO1) levels were lower at baseline in IR-R compared to T2D-R and tended to rise only in IR-R (Fig. 6, D and E). After HIIT, expression also of both p38 MAPK and p44/p42 MAPK, as inflammation mediator targets of TNFα (*37*), was lower in IR-R and in IS-NR (Fig. 6, F and G). Expression levels of microtubule-associated proteins 1A/1B light chain 3B (LC3) and ubiquitin-binding protein p62 (p62) were increased after HIIT only in IS-NR (Fig. 6, H and I).

DISCUSSION

This study found that (i) most IR but not IS humans respond to HIIT with improved insulin sensitivity, (ii) the myocellular pathways involved in insulin sensitivity (NF-κB versus nPKC) may differ upon HIIT between nondiabetic and diabetic responders, (iii) only the responders increase their circulating SEV, and (iv) the SEV proteome composition is differently affected between nondiabetic and diabetic responders (up-regulated NRF2 versus down-regulated PLC, PKA, and ERK pathways), probably in relationship to changes in muscle metabolism. First, this study showed that HIIT similarly improves whole-body, muscle maximal oxygen uptake and muscle mitochondrial mass, at least when assessed from CSA, in metabolically healthy and in IR groups (IR NDM and T2D). This is in line with the exercise-induced elevations in PGC1-α, mitochondrial density, oxidative capacity, and mitochondrial complex proteins reported for glucose-tolerant and T2D individuals (*38*, *39*). Exhaustive exercising may not only increase oxidative capacity but also cause oxidative stress with beneficial effects on mitochondrial adaptation and insulin sensitivity (*40*). The present study demonstrated that HIIT reduced the GSH/GSSG ratio in all groups and the rate of H_2O_2 production only in IR NDM and IS NDM, probably due to a greater increase in mitochondrial content based on CSA, leading to the hypothesis that GSH—as a compensatory antioxidative mechanism—is unlikely required to counteract oxidative stress under these conditions. Moreover, HIIT ameliorated peripheral and hepatic insulin sensitivity in the IR groups. Previous HIIT studies reported heterogeneous results in individuals with metabolic diseases albeit mostly using less accurate methods than the hyperinsulinemic-euglycemic clamp to assess insulin sensitivity (*41*). In contrast, a study implying a two-step clamp protocol showed that HIIT improved peripheral insulin sensitivity but not EGP in young and elderly people with similar baseline insulin sensitivity (*7*). Notably, one 8-week HIIT study found improved HOMA-IR in IR humans (*42*), and a 6-week intensive exercise intervention led to greater insulin-stimulated muscle glucose transport/phosphorylation in IR offspring of parents with T2D than in glucose-tolerant humans (*43*). These findings already

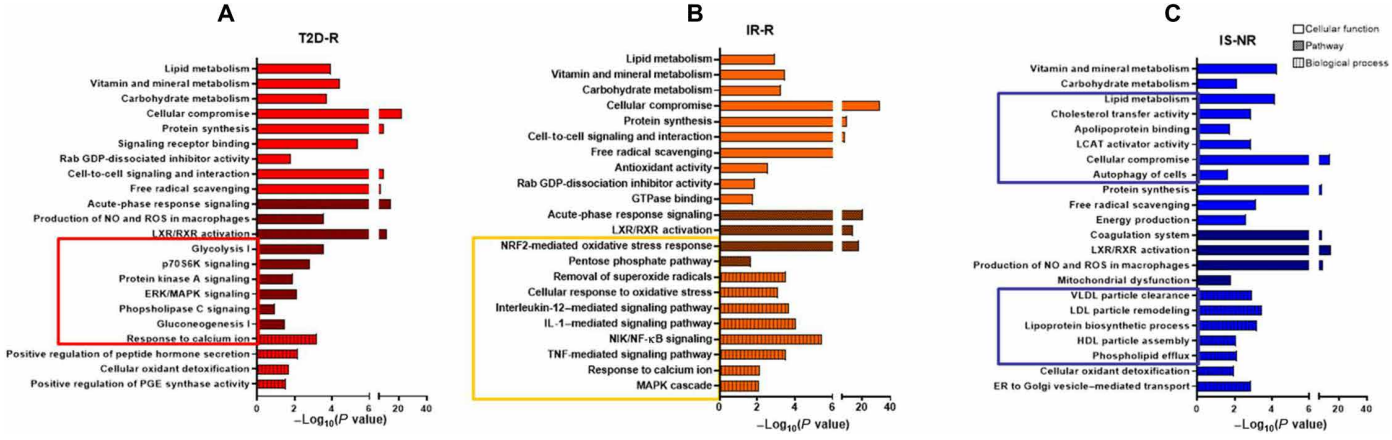

Fig. 5. HIIT differently affects the proteomic profile of SEVs in IR (IR-R and T2D-R) and IS humans. Cellular functions, pathways, and biological process of the SEV proteins regulated during exercise in T2D-R (**A**), IR-R (**B**), and IS-NR (**C**). Squares indicate the unique pathways for each group.

indicate an ability of IR individuals to (over)compensate for insulin resistance by adequate exercise training.

Notably, it has been estimated that 20% of T2D are nonresponders to exercise (*3*), and 31% do not improve their metabolic control and insulin sensitivity after hypocaloric dietary intervention (*44*). Genetic predisposition could play an important role regarding response to lifestyle interventions, as reported in several studies (*45*, *46*). For example, nonresponse among glucose-tolerant relatives of parents with T2D has been attributed to a polymorphism in the *NDUFB6* gene, which encodes a subunit of mitochondrial CI (*47*), supporting the concept of a tight association between mitochondrial function and changes in insulin sensitivity in patients with T2D (*39*). Notably, the present study found that mainly IR individuals responded to HIIT with improved insulin resistance independently of muscle mitochondrial function. In this context, another study reported that nonresponders to exercise training also had higher baseline insulin sensitivity along with different DNA methylation status and RNA expression patterns (*48*). In line, the inflammatory and metabolic responses to nutritional interventions are less impressive in people with lower cardiometabolic risk compared to individuals with the metabolic syndrome (*49*).

The present study showed that the improvement of insulin resistance upon HIIT associated with different pathways in T2D and IR NDM. More specifically, in T2D, but not in IR NDM, we found a reduction of nPKCε and θ activities. This indicates that DAG/nPKC pathway, which is well known to mediate lipid-induced insulin resistance (*25*), is down-regulated by HIIT at least in overt diabetes but not necessarily in all IR groups. In line, HIIT also led to reductions in liver fat content paralleled with enhanced hepatic insulin sensitivity in both T2D and IR NDM, and these changes were in contrast to the divergent effects of HIIT in nonalcoholic fatty liver disease (*50*, *51*).

The T2D group also showed activation of the NF-κB pathway, which is another feature of long-standing obesity and T2D (*37*). HIIT reduced NF-κB protein expression in IR NDM, but not in T2D, indicating the operation of different mechanisms of metabolic exercise response in individuals with or without diabetes. One might suggest that improvement of the more severe insulin resistance requires reduction of the lipotoxic pathways in skeletal muscle. Notably, the reduction in myocellular inflammatory pathways in IR NDM was not accompanied by any changes in circulating inflammatory markers, suggesting that low-grade (subclinical) inflammation may not be the primary interorgan cross-talk mechanism explaining HIIT-induced metabolic changes.

To elucidate other mechanisms of interorgan cross-talk mediating the metabolic effects of HIIT (*12*), we isolated circulating SEV and found that their number was already lower in IR responders than in BMI-matched IS nonresponders before exercise training. This is in contrast to a recent study reporting higher number of EV in T2D than lean healthy humans (*52*), which may be explained by the differences in BMI between the groups, since circulating EVs are significantly increased in obesity (*53*). In addition, the previous study reported an increase of total (large and small vesicles) and large EV but not specifically of SEV because of a different method of vesicle isolation.

Previous studies have only reported on the acute release of EV upon a single exercise bout in healthy mice and humans (*12*, *14*, *15*). This study shows that the 12-week HIIT induces secretion of SEV in IR humans responding with improved insulin resistance (IR-R and T2D-R). In addition, several SEV proteins regulated after HIIT overlapped with exosomal proteins released from hSkMC after EPS in vitro, supporting the concept that skeletal muscle is likely the major contributor to exercise-induced SEV release. The large skeletal muscle mass, its central involvement in exercise responses, and high secretory activity in terms of myokines may serve to support this contention (*54*).

Functional analysis of SEV proteins differentially expressed after HIIT in T2D-R indicated that SEV proteins tend to participate in the PLC, PKA, and ERK/MAPK signaling and may affect signaling pathways, i.e., nPKC activity and AMPKα, in skeletal muscle of T2D-R and lead to improved insulin sensitivity (*17*, *55*). Although we did not investigate molecular pathways in other target tissues, it is conceivable that SEVs mediate metabolic improvements also in other organs, such as liver, and contribute with its cargo to ameliorate hepatic insulin sensitivity via inhibition of PKCε and activation of AMPKα, as previously described in PKCε knockout mice (*56*) and primary hepatocytes treated with metformin (*57*). In IR-R, the SEV proteome after HIIT displayed an up-regulation of the 20*S* core proteasome complex of the noncanonical NF-κB– and TNF-mediated pathways, which reduce inflammation via degradation of NF-κB and transcriptional termination of target genes (*32*, *33*), and activation of the NRF2-mediated oxidative stress response, which potentiate antioxidative response in target tissues. Notably, skeletal muscle of IR-R showed reduced NF-κB, p38, and p44/p42 MAPK proteins

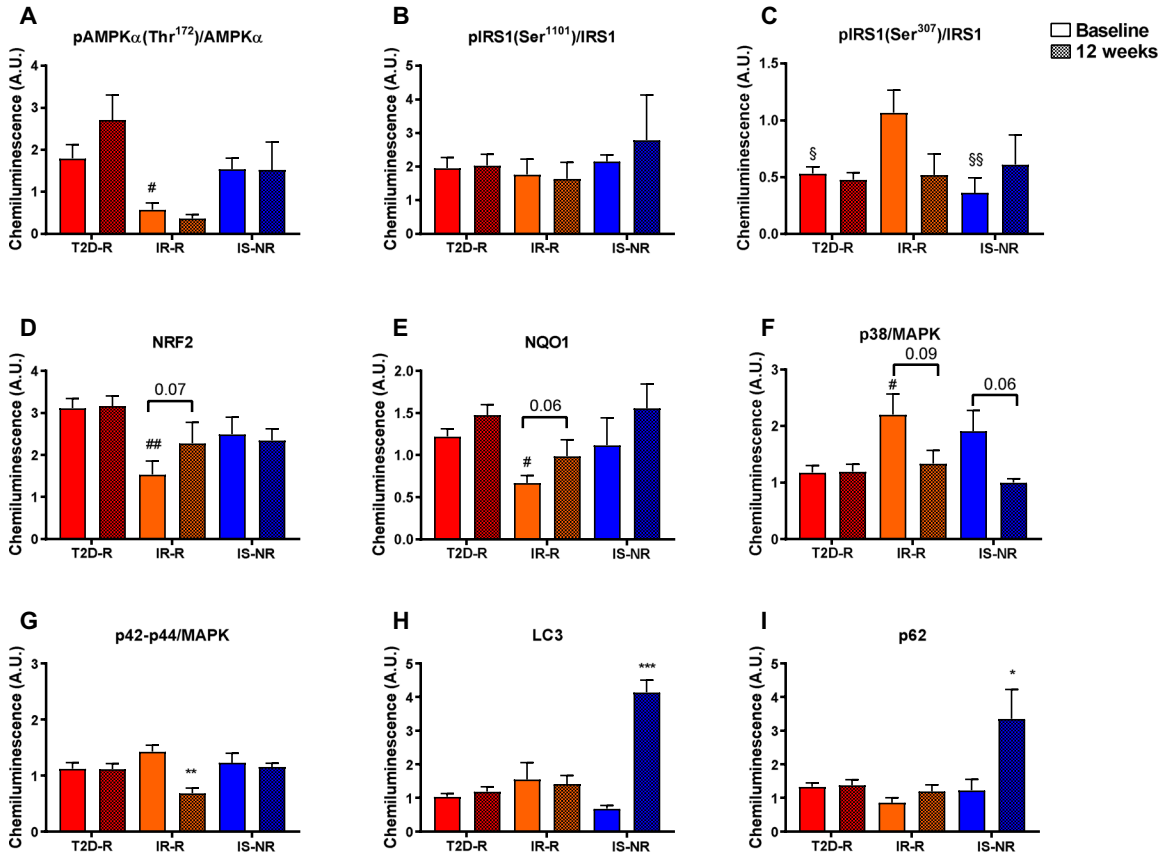

Fig. 6. Selected SEV-cargoed proteins are differentially expressed in skeletal muscle after HIIT. Western blot analysis of pAMPKα(Thr^{172})/AMPKα (#P = 0.03 T2D-R versus IR-R) (**A**), pIRS1(Ser^{1101})/IRS1 (**B**), pIRS1(Ser^{307})/IRS1 (§P = 0.02 T2D-R versus IR-R, §§P = 0.007 IR-R versus IS-NR) (**C**), NRF2 (##P = 0.001 T2D-R versus IR-R) (**D**), NQO1 (#P = 0.02 T2D-R versus IR-R) (**E**), p38/MAPK (#P = 0.01 T2D-R versus IR-R) (**F**), p42-p44/MAPK (**P = 0.002 for IR-R; P = 0.009 T2D-R versus IR-R, P = 0.02 IR-R versus IS-NR) (**G**), LC3 (***P = 0.0001 for IS-NR; P < 0.0001 IS-NR versus T2D-R and IR-R) (**H**), and p62 (*P = 0.02 for IS-NR; P = 0.003 IS-NR versus T2D-R and IR-R) (**I**) in muscle biopsies obtained from T2D-R (N = 15), IR-R (N = 9), and IS-NR (N = 7) individuals at baseline and after the 12-week HIIT. Data are expressed as means ± SEM.

and up-regulation of NRF2 and NQO1 proteins, which decrease the inhibitory Ser^{307} phosphorylation of IRS1 and protect against insulin resistance (*17*, *58*). One may hypothesize that SEV content may activate these myocellular signaling pathways and could reduce the activation of NF-κB also in liver, thereby diminishing hepatic inflammation, insulin resistance, and fat content (*59*), as observed in IR-R after HIIT.

Last, the proteome of SEV isolated from IS-NR did not reveal any significant inhibition or activation of pathways, besides cellular autophagy, in line with the nonresponder status, i.e., the absence of changes in insulin sensitivity. Notably, expression of the autophagy markers, LC3 and p62, was markedly increased after the 12-week HIIT in their skeletal muscle, which may reflect enhanced endurance performance (*60*). There are some limitations of this study. First, the associative nature of the study design makes it difficult to draw firm conclusions with respect to mechanisms of insulin sensitivity. Nevertheless, the present findings can be helpful for future mechanistic studies. Second, the absence of female participants limits the generalizability of the findings, as women can exhibit differences in muscle mass and fiber type composition as well as response to exercise interventions (*61*). However, a previous study at least reported similar changes in VO_2max, power output, and substrate oxidation upon 6 days of HIIT in both healthy men and women (*62*). Third, SEV characterization also in the other subgroups (T2D-NR, IR-NR, and IS-R) would have improved the view on the role of SEV as mediators of insulin response to exercising. However, we focused our SEV analyses on the subgroups exhibiting relevant differences from each other at baseline and after HIIT to identify specific molecular changes underlying the metabolic adaptations to exercising.

In conclusion, this study shows that (i) even highly efficient HIIT does not generally improve peripheral insulin sensitivity but allows to identify responders, who are more likely IR humans at baseline; that (ii) exercise response of insulin sensitivity relates to different mechanisms among individuals with or without T2D, i.e., reduction of myocellular lipotoxic signaling via DAG/nPKC or down-regulation of NF-κB pathways; and that (iii) different amount and proteome of circulating SEV likely contribute to the variability in metabolic exercise response. These findings might help to better understand mechanisms of lifestyle intervention and to identify previously unknown targets for the tailored prevention and treatment of insulin resistance and T2D in the concept of precision medicine but will require further studies on the underlying mechanisms.

MATERIALS AND METHODS

Study participants and study design

This study included 20 male patients with T2D and 12 age-matched IS and 11 IR glucose-tolerant male participants (NDM). All

participants underwent a screening procedure with detailed physical examination, interview, blood sampling, and spiroergometry. Exclusion criteria were performance of more than 60 min of endurance training per week; acute or chronic cardiovascular, renal, or liver diseases; use of insulin-sensitizing medication or beta-blockers; alcohol intake of more than 30 g/day; and smoking. Volunteers of the control group needed to have neither a family history of T2D nor dysglycemia during a standardized 75-g oral glucose tolerance test. All participants gave written informed consent before inclusion in the study, which was approved by the Institutional Review Board of Heinrich Heine University Düsseldorf (NCT02039934) and performed according to the World's Medical Association Declaration of Helsinki.

Exercise training protocol and diet control

All participants took part in a progressive 12-week supervised cycle ergometer training protocol of a total duration of 35 min per session consisting of four 4-min high-intensity intervals (HIIT), during which the participant trained at an intensity corresponding to 90% of their maximal heart rate as determined during a baseline spiroergometry (*63*). These intervals were interspersed by three 3-min intervals, during which the participant trained at 70% of their maximal heart rate. Exercise training sessions were repeated three times weekly on nonconsecutive days. Over the 12-week training period, we adjusted workload progressively to maintain the target heart rate. We instructed all participants to maintain their body weight (change up to 5% of initial body weight was tolerated) throughout the training period. In turn, we checked body weight every 4 weeks, and participants presenting with a 3% change of their initial body weight received adequate dietary counseling by our expert clinical nutritionists.

Spiroergometry

Each participant performed an incremental exhaustive exercise test on an electronically braked cycle ergometer (Ergoline ergometrix 900, Bitz, Germany) at 60 rpm (*64*). We determined respiratory gas exchange measurements by open-air spirometry (MasterScreen CPX; Jäger/Viasys, Hoechberg, Germany) (*65*). During exercising, we increased work rate continually by 15 W/min increments, and the incremental part of the test lasted 8 to 12 min. Blood pressure, heart rate, and a 12-lead electrocardiogram were recorded every 2 min during the test. Capillary blood was drawn from the ear every 2 min and then every minute after the anaerobic threshold for the measurement of lactate.

Hyperinsulinemic-euglycemic clamp tests

We performed two-step hyperinsulinemic-euglycemic clamp tests for the assessment of peripheral and hepatic insulin sensitivity before intervention and 72 hours after the last training session. Participants with T2D did not take their oral glucose-lowering medication for 3 days before the clamp to avoid any interference from metabolic drug effects (*66*). After withdrawal of their oral glucose-lowering medication, they performed frequent glucose self-monitoring and should contact the study team in case of blood glucose levels of >200 mg/dl, which was not required by any of the participants with T2D. We performed the clamp tests as previously described (*67*). On the day of test, participants arrived at the clinical research center at 7:00 a.m., where they received two venous catheters in the antecubital veins of both arms for blood sampling and infusions of glucose and insulin. A primed-continuous infusion of 98% enriched D-[6,6-$^2H_2$]glucose was initiated at min 0 and continued until the end of the clamp test to measure EGP. After 120 min, we administered a low-dose primed-continuous infusion [20 mU/(square meter of body surface area*minute); low insulin clamp] of insulin (Actrapid, Novo Nordisk, Copenhagen, Denmark), followed by a higher-dose primed-continuous infusion [40 mU/(square meter of body surface area*minute); high insulin clamp] from 120 to 240 min (*67*). A continuous somatostatin infusion was administered throughout the clamp to inhibit endogenous insulin secretion. We performed blood glucose measurements every 5 min and adjusted a 20% dextrose infusion labeled with D-[6,6-$^2H_2$]glucose (2% enriched) to maintain normoglycemia (5 mM). Peripheral insulin sensitivity was measured from mean whole-body glucose infusion rates (*M* value) during the last 30 min of the clamp with glucose space correction.

Laboratory measurements

We obtained all parameters in the morning of test day and after 10 hours of fasting (*64*). Blood glucose, serum TG, high- and low-density lipoproteins, and SGPT were measured on a Cobas c311 (Roche Diagnostics, Mannheim, Germany). Serum concentrations of insulin and C-peptide were measured with radioimmunoassay (Millipore, St. Charles, MO, USA) and FFA microfluorimetrically.

Proton magnetic resonance spectroscopy

Liver fat content was quantified by volume-selective proton magnetic resonance spectroscopy using a stimulation echo acquisition mode in a whole-body 3-T magnetic resonance scanner, as described (*68*). Whole-body, subcutaneous, and visceral fat mass were quantified by application of a T1-weighted axial fast spin echo (*64*, *69*).

High-resolution respirometry

We assessed mitochondrial respiration in permeabilized muscle fibers from skeletal muscle biopsies in a 2-ml chamber in an Oxygraph-2k (Oroboros Instruments, Innsbruck, Austria) (*70*). We quantified leak respiration (CI_L) after addition of pyruvate and glutamate, state 3 respiration at saturating ADP concentrations (OXPHOS, CI_P) and after succinate addition (OXPHOS, CI + II_P), leak state in the presence of oligomycin that inhibits ATP synthase (CI + II_L), electron transport (CI + II_E) capacity at optimum concentration of the uncoupler carbonyl cyanide-4-(trifluoromethoxy)phenylhydrazone to obtain maximum oxygen flux, and residual oxygen consumption by addition of antimycin A. Cytochrome c was added to test for outer mitochondrial membrane integrity, and a >10% oxygen flux was considered as cutoff. We calculated LCR from the ratio of CI + II_L/CI + II_E. We used high-resolution respirometry with Amplex Red after calibration of H_2O_2 titrations to obtain a standard curve to quantify H_2O_2 emission from permeabilized muscle fibers, by sequential addition of the following: malate, pyruvate, and glutamate to assess H_2O_2 emission by electron input through CI; succinate to determine H_2O_2 emission by electron input through CI and II (CI + II); rotenone to determine H_2O_2 emission by electron input through CII (*70*). Calibration and calculation of specific H_2O_2 emission were performed by DatLab software (DatLab 6, Oroboros Instruments, Innsbruck, Austria).

Skeletal muscle biopsy

At baseline and after the 12-week HIIT, we performed a skeletal muscle biopsy on the day of clamp procedure directly before initiation of insulin infusion. The region above the musculus vastus lateralis was anesthetized using local anesthetics (Lidocain 2%), and we

obtained 100 to 500 mg of skeletal muscle tissue using a Bergstrom needle (*25*). An aliquot of 50 mg of tissue was transferred into ice-cold biopsy preservation solution for high-resolution respirometry, and the rest was stored in liquid nitrogen and frozen at −80°C until further analysis.

Glutathione assay

In skeletal muscle samples, we quantified total glutathione and GSSG contents colorimetrically (Glutathione Colorimetric Detection Kit; Thermo Fisher Scientific, Dreieich, Germany) based on the method of Griffith (*71*) and normalized to protein concentration, which was measured in the supernatant using the BCA (bicinchoninic acid) Assay Kit (Thermo Fisher Scientific).

Citrate synthase assay

CSA was assayed spectrophotometrically by a commercially available kit (Citrate Synthase Assay Kit; Sigma-Aldrich, St. Louis, MO, USA), according to the method of Morgunov and Srere (*72*). We normalized CSA for each sample to protein concentration using the BCA Assay Kit.

Western blot

We assessed expression levels of proteins of interest with Western blot (*73*). Proteins were extracted from approximately 30 mg of frozen skeletal muscle and homogenized in 300 µl of lysis buffer [25 mM tris-hydrochloride (tris-HCl), 1 mM EDTA, 150 mM NaCl, and 0.20% NP-40] with protease (cOmplete Tablets, EASYpack, Roche Diagnostics) and phosphatase (PhosSTOP, EASYpack, Roche Diagnostics) inhibitors for extraction of total soluble proteins. Samples were shaken three times for 1 min at 20 Hz in a Tissue Lyzer and centrifuged (13,000 rpm, 15 min, 4°C) to pellet insolubilized material, nuclei, and unbroken cellular membranes. We measured activities of PKCθ and PKCε from the ratios of the protein contents in membrane and cytosol fractions upon differential centrifugation. We homogenized the tissue in 300 µl of lysis buffer A (25 mM tris-HCl, 1 mM EDTA, 150 mM NaCl, and 0.20% NP-40 with protease and phosphatase inhibitors), centrifuged the homogenate (100,000*g*, 1 hour at 4°C), and transferred the supernatant containing the cytosolic fraction to a fresh tube, while we dissolved the pellet in 110 µl of buffer B (250 mM tris-HCl, 1 mM EDTA, 0.25 mM EGTA, and 2% Triton X-100) using a homogenizer. A second centrifugation step (100,000*g*, 1 hour at 4°C) was performed, and the supernatant (membrane fraction) was collected and stored at −80°C as well.

We determined the concentration of the extracted proteins in the supernatant using the BCA Assay Kit. Aliquots of 30 µg of total proteins, as well as cytosolic and membrane fractions, were diluted four times with reducing Laemmli sample buffer containing 2-mercaptoethanol (1610747, Bio-Rad, CA, USA), boiled for 5 min at 95°C (only total and cytosolic proteins), and then loaded onto a SDS–polyacrylamide gradient gel (4 to 20% Mini-PROTEAN TGX Precast Protein Gels, Bio-Rad, CA, USA). Following electrophoresis, we performed a semi-dry blotting to a polyvinylidene difluoride membrane using the Trans-Blot Turbo Transfer System (Bio-Rad, CA, USA). After blocking the membranes for 2 hours at room temperature using the blocking solution (5% milk in tris-buffered saline with Tween), we incubated the membranes with the primary antibodies diluted 1:1000 in blocking solution in combination with the respective horseradish peroxidase (HRP)–conjugated secondary anti-rabbit antibody, diluted 1:2500, or anti-mouse diluted 1:1000. Last, we coated the membranes with Immobilon Western Chemiluminescent HRP substrate (Millipore), and we detected the proteins using a Bio-Rad ChemiDoc MP Imaging System in combination with the software ImageLab 6.0.1 (Bio-Rad 199 Laboratories) for densitometric analysis. Primary antibodies were purchased from Cell Signaling Technology: LC3 (4108); p38 MAPK (9212); p44/p42 MAPK (9102); NF-κB (8242); AMPKα (2532); phospho-AMPKα (Thr^{172}) (2535); NQO1 (3187); phospho-IRS1(Ser^{307}) (2381); phospho-IRS1(Ser^{1101}) (2385); albumin (4929); calnexin (2679); HSP70 (heat shock protein 70) (4872); GAPDH (glyceraldehyde 3-phosphate dehydrogenase) (2118) as housekeeping protein for the soluble and cytosolic fractions. p62 (610833), PKCθ (610090), and PKCε (610086) were obtained from BD Biosciences; IRS1 from Millipore (06-248); NRF2 from Santa Cruz Biotechnology (sc-365949); CD63 (ab59479) and Na^+,K^+-ATPase (Ab76020), used as loading control for the membrane fraction, from Abcam; and CD9 (EXOAB-CD9A-1-SBI) from BioCat. Data are expressed in arbitrary units and normalized to the housekeeping protein.

Cell culture of primary hSkMCs

Proliferating myoblasts of three healthy Caucasian donors [male, 16, 21, and 41 years of age (M16, M21, and M41)] were obtained to generate hSkMC (PromoCell, Heidelberg, Germany) and cultured as described (*74*). For an individual experiment, we seeded the myoblasts in six-well culture dishes and cultured to 90% confluence in α-modified Eagle's medium (αMEM)/Ham's F-12 medium (Gibco, Berlin, Germany) containing supplement for skeletal muscle cell growth medium (PromoCell). Then, we differentiated the cells in αMEM supplemented with 2% horse serum for 5 days, followed by overnight starvation in αMEM without serum. Differentiated cells were subjected to EPS cells (*75*), and after 24 hours of EPS, we isolated the SEVs from conditioned medium as reported (*76*).

SEV isolation from serum

We collected serum samples before the intervention and 72 hours after the last training and isolated SEV from serum by SEC using the IZON columns (qEV2/70 nm) coupled to successive ultracentrifugation (*77*). Briefly, we cleared the serum samples (starting material, 750 µl) at 1500*g* for 10 min followed by centrifugation at 10,000*g* for 10 min to remove particulate matter. Then, we loaded the serum supernatant into an IZON column previously equilibrated with phosphate-buffered saline (PBS). Once the serum entered the column, 50 ml of PBS was loaded on top of the column. The first 13 ml of flow-through was discarded, and the elution fractions of 14 to 21 ml were collected. We used 300 µl of PBS-eluted EV for NTA, while the rest was centrifuged at 100,000*g* for 70 min. We discarded the supernatant and lysed the transparent pellet containing SEV for Western blot and MS sample processing or resuspended it in 20 µl of PBS for analysis by TEM.

For Western blot, we dissolved the SEV pellet in reducing Laemnli buffer for calnexin, albumin, HSP70, and CD9 or Laemnli buffer without 2-mercaptoethanol for CD63; boiled it for 5 min at 95°C; and then loaded it onto a SDS–polyacrylamide gradient gel as described above. HepG2 cell lysate and serum were used as a positive control for calnexin and albumin.

Nanoparticle tracking analysis

We assessed count and size of SEV by NTA, which measures in real time the Brownian motion of vesicles resuspended in fluid. We used

a NanoSight NS300 (Malvern Panalytical) with a 488-nm laser and the NTA 3.3 software to detect the SEV by laser light scattering. Samples dissolved in PBS were diluted with 0.22-μm-filtered PBS to achieve 25 to 80 particles per frame. Data were collected from 3 × 90 s videos recorded at a constant temperature of 25°C with viscosity of 0.9 centipoise, camera level of 16, and detection threshold of 4.

Mass spectrometry

EV pellets derived from human serum samples and skeletal muscle cells were lysed in denaturing SDS buffer [62.5 mM tris-HCl (pH 6.8), 10% glycerol, 2 mM EDTA, 2% SDS, and 100 mM dithiothreitol (DTT)] and loaded onto SDS–polyacrylamide gel electrophoresis (10% polyacrylamide, 0.5 cm separation distance) as previously described (*76*). Subsequent to protein quantification of the Coomassie blue–stained protein bands against a bovine serum albumin standard, we excised bands and subjected them to in-gel protein digestion. Therefore, we washed gel slices alternately twice with 25 mM ammonium bicarbonate and 25 mM ammonium bicarbonate and 50% (v/v) acetonitrile (ACN). Protein reduction was performed in 65 mM DTT for 15 min, shaking at 350 rpm and 50°C. Proteins were then alkylated in 216 mM iodoacetamide for 15 min in the dark at room temperature. Followed by an additional washing step [25 mM ammonium bicarbonate, 25 mM ammonium bicarbonate, and 50% ACN (v/v)], gel slices were shrunk in 100% (v/v) ACN. Digestion was performed with 100 ng of trypsin (Promega) in 25 mM ammonium bicarbonate and 2% (v/v) ACN overnight at 37°C. Resulting peptides were eluted first with 1% (v/v) trifluoroacetic acid (TFA) followed by elution with 0.1% TFA/90% (v/v) ACN and lyophilization. For MS analysis, we reconstituted lyophilized peptides in 1% TFA (v/v) including iRT (indexed retention time) peptides (Biognosys) and separated them by liquid chromatography (Ultimate 3000, Thermo Fisher Scientific) using an EASY-Spray ion source equipped to an Orbitrap Fusion Lumos mass spectrometer (Thermo Fisher Scientific). Peptides were trapped and desalted on an Acclaim PepMap C18-LC-column (ID: 75 μm, 2 cm length; Thermo Fisher Scientific) and subsequently separated via EASY-Spray C18 column (ES803; ID: 50 cm by 75 μm inner diameter; Thermo Fisher Scientific) using a 100-min linear gradient from buffer A (0.1% formic acid) to 4 to 34% buffer B (80% ACN and 0.1% formic acid) at a flow rate of 300 nl/min, followed by a 20-min linear gradient increasing buffer B to 50% and a 1-min linear gradient increasing buffer B to 90%. Column temperature was set to 40°C.

We acquired MS data for generating spectral libraries on an Orbitrap Fusion Lumos instrument (Thermo Fisher Scientific) operated in data-dependent mode. MS spectra were obtained at 120,000 resolution (3-s cycle time), *m/z* (mass/charge ratio) range of 350 to 1600, and a target value of 4^5 ions with maximum injection time of 50 ms. For fragmentation precursor, we set the selection filter to charge state between 2 and 7, dynamic exclusion of 30 s, and intensity threshold of 2.5^4. Fragmentation of precursors was performed with an isolation window (*m/z*) of 1.2, HCD (higher-energy collisional dissociation) energy of 32%, Orbitrap resolution of 15,000, and an ion target value of 1.0^5 with maximum injection time of 50 ms.

We acquired MS data for label-free quantification in a DIA (data-independent acquisition) mode. Full-scan MS spectra were obtained at 120,000 resolution, *m/z* range of 400 to 1200, AGC (automatic gain control) target value of 5^5, and maximum injection time of 50 ms. Fragmentation was performed with HCD energy of 32% in 34 windows covering the range from 400 to 1200 with a segment width of 24.5 (*m/z*), Orbitrap resolution of 30,000, AGC target of 1.0^6, scan range from 200 to 2000 (*m/z*), and a maximal injection time of 60 ms.

Analysis of MS data

We imported DDA (data-dependent acquisition) and DIA data into Spectronaut Pulsar (Version 12, Biognosys) to generate a sample-specific library using the default settings [modifications: carbamidomethyl (C) (fixed); oxidation (M), acetyl (protein N-term) (variable); enzyme: trypsin/P; maximum missed cleavages: 2] (*78*). Pulsar search was performed against a human FASTA file (UniProtKB database, reviewed SwissProt, *Homo sapiens* TaxID 9096 canonical and isoforms, downloaded July 2018), and we filtered results by a false discovery rate (FDR) of 1% on precursor and protein group level ($q < 0.01$).

For quantitative analysis, we analyzed the DIA data in Spectronaut (version 12, Biognosys) using the generated library (obtained from the corresponding DDA and DIA runs) with default settings. We created the candidate list using an average $\log_2$ ratio ≤ 0.58 and $q \leq 0.05$.

Transmission electron microscopy

We transferred SEVs (5 μl) to Ni 400 mesh formvar carbon-coated grids for TEM analysis, incubated for 10 s, washed three times with PBS, and negatively stained by applying three times 1.5% (w/v) uranylacetate solution for a few seconds. Last, we dried the grids and performed TEM using an H-7100 (Hitachi, Japan) transmission electron microscope at 80 kV.

Bioinformatic analysis

The protein information was extracted from Swiss-Prot database (www.uniprot.org/). The prediction of a secretory SP was performed with the server SignalP 4.1 using as cutoff 0.450 (*79*, *80*), and we further analyzed the proteins without a SP with SecretomeP 2.0 to identify nonclassically secreted proteins (score > 0.6) (*79*). The comparison between our study and the vesicle database Vesiclepedia was performed using FunRich (v3.1.3; released on 2018) (*80*). We performed GO enrichment analysis of the SEV proteins regulated during exercise for CC (GO-CC), GO-MF, and GO-BP versus annotations derived from UniProt, with cutoff enriched $P < 0.05$ (B-H–corrected FDR value).

In addition, we uploaded the proteomic dataset, with UniProt identifiers, FC 12-week HIIT versus baseline and *q* value of each comparison, into IPA (Ingenuity, Qiagen, Hilden, Germany) for core analysis and overlaid with the ingenuity pathways knowledge-base to categorize the SEV-cargoed proteins in biological functions and pathways. IPA also predicted the upstream regulators for the proteins in the dataset, which are responsible for the pathways and networks most relevant to the dataset.

Statistical analysis

We present data as means ± SEM or median (first and third quartiles), as appropriate. Variables with a skewed distribution (*M* value, TG, liver fat content, SEV number, and protein levels) were log-transformed before analysis. We performed analysis of covariance (ANCOVA)–like linear regression analyses of baseline to 12-week HIIT changes allowing for different residual variances between the investigated groups, one-way or two-way analysis of variance (ANOVA), and *t* tests. We used logistic regression analysis to estimate the

probability of responder status in each group and to investigate associations between PKC activity and *M* value.

Analysis in IPA was performed using the B-H method of multiple testing correction, based on the Fisher's exact test *P* value with a threshold value of 0.05, and the *z* score algorithm, which predicts the activation or inhibition of pathways and functions after HIIT according to the molecule expression changes in our dataset. We considered only functions and pathways with a *z* score of >2 or <2. We used the B-H–corrected *P* value (threshold, <0.05) also to determine statistical significance enriched GO terms. We removed duplicate or highly similar GO terms and selected only those with the highest statistical power or with the highest number of genes in the background dataset. GraphPad Prism 8 was used to plot the graphs when comparing datasets (GraphPad Software Inc).

SUPPLEMENTARY MATERIALS

Supplementary material for this article is available at https://science.org/doi/10.1126/sciadv.abi9551

View/request a protocol for this paper from *Bio-protocol*.

REFERENCES AND NOTES

1. A. Chudyk, R. J. Petrella, Effects of exercise on cardiovascular risk factors in type 2 diabetes: A meta-analysis. *Diabetes Care* **34**, 1228–1237 (2011).
2. S. R. Colberg, R. J. Sigal, J. E. Yardley, M. C. Riddell, D. W. Dunstan, P. C. Dempsey, E. S. Horton, K. Castorino, D. F. Tate, Physical activity/exercise and diabetes: A position statement of the american diabetes association. *Diabetes Care* **39**, 2065–2079 (2016).
3. N. A. Stephens, L. M. Sparks, Resistance to the beneficial effects of exercise in type 2 diabetes: Are some individuals programmed to fail? *J. Clin. Endocrinol. Metab.* **100**, 43–52 (2015).
4. G. Kacerovsky-Bielesz, M. Kacerovsky, M. Chmelik, M. Farukuoye, C. Ling, R. Pokan, H. Tschan, J. Szendroedi, A. I. Schmid, S. Gruber, C. Herder, M. Wolzt, E. Moser, G. Pacini, G. Smekal, L. Groop, M. Roden, A single nucleotide polymorphism associates with the response of muscle ATP synthesis to long-term exercise training in relatives of type 2 diabetic humans. *Diabetes Care* **35**, 350–357 (2012).
5. L. M. Sparks, Exercise training response heterogeneity: Physiological and molecular insights. *Diabetologia* **60**, 2329–2336 (2017).
6. M. J. Gibala, J. P. Little, M. J. Macdonald, J. A. Hawley, Physiological adaptations to low-volume, high-intensity interval training in health and disease. *J. Physiol.* **590**, 1077–1084 (2012).
7. M. M. Robinson, S. Dasari, A. R. Konopka, M. L. Johnson, S. Manjunatha, R. R. Esponda, R. E. Carter, I. R. Lanza, K. S. Nair, Enhanced protein translation underlies improved metabolic and physical adaptations to different exercise training modes in young and old humans. *Cell Metab.* **25**, 581–592 (2017).
8. B. A. Irving, K. R. Short, K. S. Nair, C. S. Stump, Nine days of intensive exercise training improves mitochondrial function but not insulin action in adult offspring of mothers with type 2 diabetes. *J. Clin. Endocrinol. Metab.* **96**, E1137–E1141 (2011).
9. C. Herder, M. Carstensen, D. M. Ouwens, Anti-inflammatory cytokines and risk of type 2 diabetes. *Diabetes Obes. Metab.* **15** (Suppl. 3), 39–50 (2013).
10. S. Molnos, S. Wahl, M. Haid, E. M. W. Eekhoff, R. Pool, A. Floegel, J. Deelen, D. Much, C. Prehn, M. Breier, H. H. Draisma, N. van Leeuwen, A. M. C. Simonis-Bik, A. Jonsson, G. Willemsen, W. Bernigau, R. Wang-Sattler, K. Suhre, A. Peters, B. Thorand, C. Herder, W. Rathmann, M. Roden, C. Gieger, M. H. H. Kramer, D. van Heemst, H. K. Pedersen, V. Gudmundsdottir, M. B. Schulze, T. Pischon, E. J. C. de Geus, H. Boeing, D. I. Boomsma, A. G. Ziegler, P. E. Slagboom, S. Hummel, M. Beekman, H. Grallert, S. Brunak, M. I. McCarthy, R. Gupta, E. R. Pearson, J. Adamski, L. M. t. Hart, Metabolite ratios as potential biomarkers for type 2 diabetes: A DIRECT study. *Diabetologia* **61**, 117–129 (2018).
11. S. Vasu, K. Kumano, C. M. Darden, I. Rahman, M. C. Lawrence, B. Naziruddin, MicroRNA signatures as future biomarkers for diagnosis of diabetes states. *Cell* **8**, 1533 (2019).
12. A. Safdar, A. Saleem, M. A. Tarnopolsky, The potential of endurance exercise-derived exosomes to treat metabolic diseases. *Nat. Rev. Endocrinol.* **12**, 504–517 (2016).
13. C. Thery, K. W. Witwer, E. Aikawa, M. J. Alcaraz, J. D. Anderson, R. Andriantsitohaina, A. Antoniou, T. Arab, F. Archer, G. K. Atkin-Smith, D. C. Ayre, J.-M. Bach, D. Bachurski, H. Baharvand, L. Balaj, S. Baldacchino, N. N. Bauer, A. A. Baxter, M. Bebawy, C. Beckham, A. B. Zavec, A. Benmoussa, A. C. Berardi, P. Bergese, E. Bielska, C. Blenkiron, S. Bobis-Wozowicz, E. Boilard, W. Boireau, A. Bongiovanni, F. E. Borràs, S. Bosch, C. M. Boulanger, X. Breakefield, A. M. Breglio, M. Á. Brennan, D. R. Brigstock, A. Brisson, M. L. Broekman, J. F. Bromberg, P. Bryl-Górecka, S. Buch, A. H. Buck, D. Burger, S. Busatto, D. Buschmann, B. Bussolati, E. I. Buzás, J. B. Byrd, G. Camussi, D. R. Carter, S. Caruso, L. W. Chamley, Y.-T. Chang, C. Chen, S. Chen, L. Cheng, A. R. Chin, A. Clayton, S. P. Clerici, A. Cocks, E. Cocucci, R. J. Coffey, A. Cordeiro-da-Silva, Y. Couch, F. A. Coumans, B. Coyle, R. Crescitelli, M. F. Criado, C. D'Souza-Schorey, S. Das, A. D. Chaudhuri, P. de Candia, E. F. De Santana, O. De Wever, H. A. Del Portillo, T. Demaret, S. Deville, A. Devitt, B. Dhondt, D. D. Vizio, L. C. Dieterich, V. Dolo, A. P. D. Rubio, M. Dominici, M. R. Dourado, T. A. Driedonks, F. V. Duarte, H. M. Duncan, R. M. Eichenberger, K. Ekström, S. E. Andaloussi, C. Elie-Caille, U. Erdbrügger, J. M. Falcón-Pérez, F. Fatima, J. E. Fish, M. Flores-Bellver, A. Försönits, A. Frelet-Barrand, F. Fricke, G. Fuhrmann, S. Gabrielsson, A. Gámez-Valero, C. Gardiner, K. Gärtner, R. Gaudin, Y. S. Gho, B. Giebel, C. Gilbert, M. Gimona, I. Giusti, D. C. Goberdhan, A. Görgens, S. M. Gorski, D. W. Greening, J. C. Gross, A. Gualerzi, G. N. Gupta, D. Gustafson, A. Handberg, R. A. Haraszti, P. Harrison, H. Hegyesi, A. Hendrix, A. F. Hill, F. H. Hochberg, K. F. Hoffmann, B. Holder, H. Holthofer, B. Hosseinkhani, G. Hu, Y. Huang, V. Huber, S. Hunt, A. G.-E. Ibrahim, T. Ikezu, J. M. Inal, M. Isin, A. Ivanova, H. K. Jackson, S. Jacobsen, S. M. Jay, M. Jayachandran, G. Jenster, L. Jiang, S. M. Johnson, J. C. Jones, A. Jong, T. Jovanovic-Talisman, S. Jung, R. Kalluri, S.-I. Kano, S. Kaur, Y. Kawamura, E. T. Keller, D. Khamari, E. Khomyakova, A. Khvorova, P. Kierulf, K. P. Kim, T. Kislinger, M. Klingeborn, D. J. Klinke II, M. Kornek, M. M. Kosanović, Á. F. Kovács, E.-M. Krämer-Albers, S. Krasemann, M. Krause, I. V. Kurochkin, G. D. Kusuma, S. Kuypers, S. Laitinen, S. M. Langevin, L. R. Languino, J. Lannigan, C. Lässer, L. C. Laurent, G. Lavieu, E. Lázaro-Ibáñez, S. L. Lay, M.-S. Lee, Y. X. F. Lee, D. S. Lemos, M. Lenassi, A. Leszczynska, I. T. Li, K. Liao, S. F. Libregts, E. Ligeti, R. Lim, S. K. Lim, A. Linē, K. Linnemannstöns, A. Llorente, C. A. Lombard, M. J. Lorenowicz, Á. M. Lörincz, J. Lötvall, J. Lovett, M. C. Lowry, X. Loyer, Q. Lu, B. Lukomska, T. R. Lunavat, S. L. Maas, H. Malhi, A. Marcilla, J. Mariani, J. Mariscal, E. S. Martens-Uzunova, L. Martin-Jaular, M. C. Martinez, V. R. Martins, M. Mathieu, S. Mathivanan, M. Maugeri, L. K. M. Ginnis, M. J. M. Vey, D. G. Meckes Jr., K. L. Meehan, I. Mertens, V. R. Minciacchi, A. Möller, M. M. Jørgensen, A. Morales-Kastresana, J. Morhayim, F. Mullier, M. Muraca, L. Musante, V. Mussack, D. C. Muth, K. H. Myburgh, T. Najrana, M. Nawaz, I. Nazarenko, P. Nejsum, C. Neri, T. Neri, R. Nieuwland, L. Nimrichter, J. P. Nolan, E. Nm Nolte-'t Hoen, N. N. Hooten, L. O'Driscoll, T. O'Grady, A. O'Loghlen, T. Ochiya, M. Olivier, A. Ortiz, L. A. Ortiz, X. Osteikoetxea, O. Østergaard, M. Ostrowski, J. Park, D. M. Pegtel, H. Peinado, F. Perut, M. W. Pfaffl, D. G. Phinney, B. C. Pieters, R. C. Pink, D. S. Pisetsky, E. Pogge von Strandmann, I. Polakovicova, I. K. Poon, B. H. Powell, I. Prada, L. Pulliam, P. Quesenberry, A. Radeghieri, R. L. Raffai, S. Raimondo, J. Rak, M. I. Ramirez, G. Raposo, M. S. Rayyan, N. Regev-Rudzki, F. L. Ricklefs, P. D. Robbins, D. D. Roberts, S. C. Rodrigues, E. Rohde, S. Rome, K. M. Rouschop, A. Rughetti, A. E. Russell, P. Saá, S. Sahoo, E. Salas-Huenuleo, C. Sánchez, J. A. Saugstad, M. J. Saul, R. M. Schiffelers, R. Schneider, T. H. Schøyen, A. Scott, E. Shahaj, S. Sharma, O. Shatnyeva, F. Shekari, G. V. Shelke, A. K. Shetty, K. Shiba, P. R.-M. Siljander, A. M. Silva, A. Skowronek, O. L. Snyder II, R. P. Soares, B. W. Sódar, C. Soekmadji, J. Sotillo, P. D. Stahl, W. Stoorvogel, S. L. Stott, E. F. Strasser, S. Swift, H. Tahara, M. Tewari, K. Timms, S. Tiwari, R. Tixeira, M. Tkach, W. S. Toh, R. Tomasini, A. C. Torrecilhas, J. P. Tosar, V. Toxavidis, L. Urbanelli, P. Vader, B. W. M. van Balkom, S. G. van der Grein, J. Van Deun, M. J. C. van Herwijnen, K. Van Keuren-Jensen, G. van Niel, M. E. van Royen, A. J. van Wijnen, M. H. Vasconcelos, I. J. Vechetti Jr., T. D. Veit, L. J. Vella, É. Velot, F. J. Verweij, B. Vestad, J. L. Viñas, T. Visnovitz, K. V. Vukman, J. Wahlgren, D. C. Watson, M. H. Wauben, A. Weaver, J. P. Webber, V. Weber, A. M. Wehman, D. J. Weiss, J. A. Welsh, S. Wendt, A. M. Wheelock, Z. Wiener, L. Witte, J. Wolfram, A. Xagorari, P. Xander, J. Xu, X. Yan, M. Yáñez-Mó, H. Yin, Y. Yuana, V. Zappulli, J. Zarubova, V. Žėkas, J.-Y. Zhang, Z. Zhao, L. Zheng, A. R. Zheutlin, A. M. Zickler, P. Zimmermann, A. M. Zivkovic, D. Zocco, E. K. Zuba-Surma, Minimal information for studies of extracellular vesicles 2018 (MISEV2018): A position statement of the International Society for Extracellular Vesicles and update of the MISEV2014 guidelines. *J. Extracell. Vesicles* **7**, 1535750 (2018).
14. C. Fruhbeis, S. Helmig, S. Tug, P. Simon, E. M. Kramer-Albers, Physical exercise induces rapid release of small extracellular vesicles into the circulation. *J. Extracell. Vesicles* **4**, 28239 (2015).
15. M. Whitham, B. L. Parker, M. Friedrichsen, J. R. Hingst, M. Hjorth, W. E. Hughes, C. L. Egan, L. Cron, K. I. Watt, R. P. Kuchel, N. Jayasooriah, E. Estevez, T. Petzold, C. M. Suter, P. Gregorevic, B. Kiens, E. A. Richter, D. E. James, J. F. P. Wojtaszewski, M. A. Febbraio, Extracellular vesicles provide a means for tissue crosstalk during exercise. *Cell Metab.* **27**, 237–251.e4 (2018).
16. L. A. Mulcahy, R. C. Pink, D. R. Carter, Routes and mechanisms of extracellular vesicle uptake. *J. Extracell. Vesicles* **3**, 24641 (2014).
17. M. Roden, G. I. Shulman, The integrative biology of type 2 diabetes. *Nature* **576**, 51–60 (2019).
18. E. Ferrannini, G. Buzzigoli, R. Bonadonna, M. A. Giorico, M. Oleggini, L. Graziadei, R. Pedrinelli, L. Brandi, S. Bevilacqua, Insulin resistance in essential hypertension. *N. Engl. J. Med.* **317**, 350–357 (1987).
19. J. L. Welton, J. P. Webber, L. A. Botos, M. Jones, A. Clayton, Ready-made chromatography columns for extracellular vesicle isolation from plasma. *J. Extracell. Vesicles* **4**, 27269 (2015).
20. Y. Karusheva, T. Koessler, K. Strassburger, D. Markgraf, L. Mastrototaro, T. Jelenik, M. C. Simon, D. Pesta, O. P. Zaharia, K. Bódis, F. Bärenz, D. Schmoll, M. Wolkersdorfer,

A. Tura, G. Pacini, V. Burkart, K. Müssig, J. Szendroedi, M. Roden, Short-term dietary reduction of branched-chain amino acids reduces meal-induced insulin secretion and modifies microbiome composition in type 2 diabetes: A randomized controlled crossover trial. *Am. J. Clin. Nutr.* **110**, 1098–1107 (2019).
21. S. Larsen, J. Nielsen, C. N. Hansen, L. B. Nielsen, F. Wibrand, N. Stride, H. D. Schroder, R. Boushel, J. W. Helge, F. Dela, M. Hey-Mogensen, Biomarkers of mitochondrial content in skeletal muscle of healthy young human subjects. *J. Physiol.* **590**, 3349–3360 (2012).
22. K. Aquilano, S. Baldelli, M. R. Ciriolo, Glutathione: New roles in redox signaling for an old antioxidant. *Front. Pharmacol.* **5**, 196 (2014).
23. S. E. Shoelson, J. Lee, A. B. Goldfine, Inflammation and insulin resistance. *J. Clin. Invest.* **116**, 1793–1801 (2006).
24. J. Szendroedi, E. Phielix, M. Roden, The role of mitochondria in insulin resistance and type 2 diabetes mellitus. *Nat. Rev. Endocrinol.* **8**, 92–103 (2011).
25. J. Szendroedi, T. Yoshimura, E. Phielix, C. Koliaki, M. Marcucci, D. Zhang, T. Jelenik, J. Müller, C. Herder, P. Nowotny, G. I. Shulman, M. Roden, Role of diacylglycerol activation of PKCθ in lipid-induced muscle insulin resistance in humans. *Proc. Natl. Acad. Sci. U.S.A.* **111**, 9597–9602 (2014).
26. S. E. Shoelson, J. Lee, M. Yuan, Inflammation and the IKKβ/IκB/NF-κB axis in obesity- and diet-induced insulin resistance. *Int. J. Obes. Relat. Metab. Disord.* **27**, S49–S52 (2003).
27. S. K. Powers, E. E. Talbert, P. J. Adhihetty, Reactive oxygen and nitrogen species as intracellular signals in skeletal muscle. *J. Physiol.* **589**, 2129–2138 (2011).
28. M. Smolarz, M. Pietrowska, N. Matysiak, L. Mielanczyk, P. Widlak, Proteome profiling of exosomes purified from a small amount of human serum: The problem of co-purified serum components. *Proteomes* **7**, 18 (2019).
29. S. Mathivanan, H. Ji, R. J. Simpson, Exosomes: Extracellular organelles important in intercellular communication. *J. Proteomics* **73**, 1907–1920 (2010).
30. N. Kurgan, N. Noaman, M. R. Pergande, S. M. Cologna, J. R. Coorssen, P. Klentrou, Changes to the human serum proteome in response to high intensity interval exercise: A sequential top-down proteomic analysis. *Front. Physiol.* **10**, 362 (2019).
31. R. Barazzoni, E. Kiwanuka, M. Zanetti, M. Cristini, M. Vettore, P. Tessari, Insulin acutely increases fibrinogen production in individuals with type 2 diabetes but not in individuals without diabetes. *Diabetes* **52**, 1851–1856 (2003).
32. S. Saccani, I. Marazzi, A. A. Beg, G. Natoli, Degradation of promoter-bound p65/RelA is essential for the prompt termination of the nuclear factor κB response. *J. Exp. Med.* **200**, 107–113 (2004).
33. P. E. Collins, I. Mitxitorena, R. J. Carmody, The ubiquitination of NF-κB subunits in the control of transcription. *Cell* **5**, 23 (2016).
34. R. C. Stanton, Glucose-6-phosphate dehydrogenase, NADPH, and cell survival. *IUBMB Life* **64**, 362–369 (2012).
35. A. Perez-Lopez, M. Martin-Rincon, A. Santana, I. Perez-Suarez, C. Dorado, J. A. L. Calbet, D. Morales-Alamo, Antioxidants facilitate high-intensity exercise IL-15 expression in skeletal muscle. *Int. J. Sports Med.* **40**, 16–22 (2019).
36. A. Savina, M. Furlan, M. Vidal, M. I. Colombo, Exosome release is regulated by a calcium-dependent mechanism in K562 cells. *J. Biol. Chem.* **278**, 20083–20090 (2003).
37. H. Wu, C. M. Ballantyne, Skeletal muscle inflammation and insulin resistance in obesity. *J. Clin. Invest.* **127**, 43–54 (2017).
38. J. P. Little, A. Safdar, G. P. Wilkin, M. A. Tarnopolsky, M. J. Gibala, A practical model of low-volume high-intensity interval training induces mitochondrial biogenesis in human skeletal muscle: Potential mechanisms. *J. Physiol.* **588**, 1011–1022 (2010).
39. F. G. Toledo, E. V. Menshikova, V. B. Ritov, K. Azuma, Z. Radikova, J. De Lany, D. E. Kelley, Effects of physical activity and weight loss on skeletal muscle mitochondria and relationship with glucose control in type 2 diabetes. *Diabetes* **56**, 2142–2147 (2007).
40. D. Pesta, M. Roden, The janus head of oxidative stress in metabolic diseases and during physical exercise. *Curr. Diab. Rep.* **17**, 41 (2017).
41. S. Cassidy, C. Thoma, D. Houghton, M. I. Trenell, High-intensity interval training: A review of its impact on glucose control and cardiometabolic health. *Diabetologia* **60**, 7–23 (2017).
42. M. A. d. Matos, D. V. Vieira, K. C. Pinhal, J. F. Lopes, M. F. Dias-Peixoto, J. R. Pauli, F. de Castro Magalhães, J. P. Little, E. Rocha-Vieira, F. T. Amorim, High-intensity interval training improves markers of oxidative metabolism in skeletal muscle of individuals with obesity and insulin resistance. *Front. Physiol.* **9**, 1451 (2018).
43. G. Perseghin, T. B. Price, K. F. Petersen, M. Roden, G. W. Cline, K. Gerow, D. L. Rothman, G. I. Shulman, Increased glucose transport-phosphorylation and muscle glycogen synthesis after exercise training in insulin-resistant subjects. *N. Engl. J. Med.* **335**, 1357–1362 (1996).
44. R. Taylor, A. al-Mrabeh, S. Zhyzhneuskaya, C. Peters, A. C. Barnes, B. S. Aribisala, K. G. Hollingsworth, J. C. Mathers, N. Sattar, M. E. J. Lean, Remission of human type 2 diabetes requires decrease in liver and pancreas fat content but is dependent upon capacity for β cell recovery. *Cell Metab.* **28**, 667 (2018).
45. C. Pickering, J. Kiely, Exercise genetics: Seeking clarity from noise. *BMJ Open Sport Exerc. Med.* **3**, e000309 (2017).
46. P. An, M. Teran-Garcia, T. Rice, T. Rankinen, S. J. Weisnagel, R. N. Bergman, R. C. Boston, S. Mandel, D. Stefanovski, A. S. Leon, J. S. Skinner, D. C. Rao, C. Bouchard; HERITAGE Family Study, Genome-wide linkage scans for prediabetes phenotypes in response to 20 weeks of endurance exercise training in non-diabetic whites and blacks: The HERITAGE Family Study. *Diabetologia* **48**, 1142–1149 (2005).
47. G. Kacerovsky-Bielesz, M. Chmelik, C. Ling, R. Pokan, J. Szendroedi, M. Farukuoye, M. Kacerovsky, A. I. Schmid, S. Gruber, M. Wolzt, E. Moser, G. Pacini, G. Smekal, L. Groop, M. Roden, Short-term exercise training does not stimulate skeletal muscle ATP synthesis in relatives of humans with type 2 diabetes. *Diabetes* **58**, 1333–1341 (2009).
48. N. A. Stephens, B. Brouwers, A. M. Eroshkin, F. Yi, H. H. Cornnell, C. Meyer, B. H. Goodpaster, R. E. Pratley, S. R. Smith, L. M. Sparks, Exercise response variations in skeletal muscle PCr recovery rate and insulin sensitivity relate to muscle epigenomic profiles in individuals with type 2 diabetes. *Diabetes Care* **41**, 2245–2254 (2018).
49. M. Monfort-Pires, S. R. Ferreira, Inflammatory and metabolic responses to dietary intervention differ among individuals at distinct cardiometabolic risk levels. *Nutrition* **33**, 331–337 (2017).
50. K. Hallsworth, C. Thoma, K. G. Hollingsworth, S. Cassidy, Q. M. Anstee, C. P. Day, M. I. Trenell, Modified high-intensity interval training reduces liver fat and improves cardiac function in non-alcoholic fatty liver disease: A randomized controlled trial. *Clin. Sci. (Lond.)* **129**, 1097–1105 (2015).
51. B. Brouwers, V. B. Schrauwen-Hinderling, T. Jelenik, A. Gemmink, L. M. Sparks, B. Havekes, Y. Bruls, D. Dahlmans, M. Roden, M. K. C. Hesselink, P. Schrauwen, Exercise training reduces intrahepatic lipid content in people with and people without nonalcoholic fatty liver. *Am. J. Physiol. Endocrinol. Metab.* **314**, E165–E173 (2018).
52. D. W. Freeman, N. N. Hooten, E. Eitan, J. Green, N. A. Mode, M. Bodogai, Y. Zhang, E. Lehrmann, A. B. Zonderman, A. Biragyn, J. Egan, K. G. Becker, M. P. Mattson, N. Ejiogu, M. K. Evans, Altered extracellular vesicle concentration, cargo, and function in diabetes. *Diabetes* **67**, 2377–2388 (2018).
53. J. Amosse, M. Durcin, M. Malloci, L. Vergori, A. Fleury, F. Gagnadoux, S. Dubois, G. Simard, J. Boursier, O. Hue, M. C. Martinez, R. Andriantsitohaina, S. Le Lay, Phenotyping of circulating extracellular vesicles (EVs) in obesity identifies large EVs as functional conveyors of macrophage migration inhibitory factor. *Mol. Metab.* **18**, 134–142 (2018).
54. B. K. Pedersen, Muscle as a secretory organ. *Compr. Physiol.* **3**, 1337–1362 (2013).
55. Y. Arkun, Dynamic modeling and analysis of the cross-talk between insulin/AKT and MAPK/ERK signaling pathways. *PLOS ONE* **11**, e0149684 (2016).
56. C. Schmitz-Peiffer, D. R. Laybutt, J. G. Burchfield, E. Gurisik, S. Narasimhan, C. J. Mitchell, D. J. Pedersen, U. Braun, G. J. Cooney, M. Leitges, T. J. Biden, Inhibition of PKCepsilon improves glucose-stimulated insulin secretion and reduces insulin clearance. *Cell Metab.* **6**, 320–328 (2007).
57. L. He, E. Chang, J. Peng, H. An, S. M. McMillin, S. Radovick, C. A. Stratakis, F. E. Wondisford, Activation of the cAMP-PKA pathway antagonizes metformin suppression of hepatic glucose production. *J. Biol. Chem.* **291**, 10562–10570 (2016).
58. A. Bloch-Damti, R. Potashnik, P. Gual, Y. le Marchand-Brustel, J. F. Tanti, A. Rudich, N. Bashan, Differential effects of IRS1 phosphorylated on Ser307 or Ser632 in the induction of insulin resistance by oxidative stress. *Diabetologia* **49**, 2463–2473 (2006).
59. D. Cai, M. Yuan, D. F. Frantz, P. A. Melendez, L. Hansen, J. Lee, S. E. Shoelson, Local and systemic insulin resistance resulting from hepatic activation of IKK-β and NF-κB. *Nat. Med.* **11**, 183–190 (2005).
60. A. Vainshtein, D. A. Hood, The regulation of autophagy during exercise in skeletal muscle. *J. Appl. Physiol.* **120**, 664–673 (2016).
61. J. S. Woo, C. Derleth, J. R. Stratton, W. C. Levy, The influence of age, gender, and training on exercise efficiency. *J. Am. Coll. Cardiol.* **47**, 1049–1057 (2006).
62. T. A. Astorino, R. P. Allen, D. W. Roberson, M. Jurancich, R. Lewis, K. McCarthy, E. Trost, Adaptations to high-intensity training are independent of gender. *Eur. J. Appl. Physiol.* **111**, 1279–1286 (2011).
63. U. Wisløff, A. Støylen, J. P. Loennechen, M. Bruvold, Ø. Rognmo, P. M. Haram, A. E. Tjønna, J. Helgerud, S. A. Slørdahl, S. J. Lee, V. Videm, A. Bye, G. L. Smith, S. M. Najjar, Ø. Ellingsen, T. Skjærpe, Superior cardiovascular effect of aerobic interval training versus moderate continuous training in heart failure patients: A randomized study. *Circulation* **115**, 3086–3094 (2007).
64. J. Szendroedi, A. Saxena, K. S. Weber, K. Strassburger, C. Herder, V. Burkart, B. Nowotny, A. Icks, O. Kuss, D. Ziegler, H. Al-Hasani, K. Müssig, M. Roden; GDS Group, Cohort profile: The German diabetes study (GDS). *Cardiovasc. Diabetol.* **15**, 59 (2016).
65. M. Apostolopoulou, K. Strassburger, C. Herder, B. Knebel, J. Kotzka, J. Szendroedi, M. Roden; GDS group, Metabolic flexibility and oxidative capacity independently associate with insulin sensitivity in individuals with newly diagnosed type 2 diabetes. *Diabetologia* **59**, 2203–2207 (2016).
66. S. Gancheva, M. Ouni, T. Jelenik, C. Koliaki, J. Szendroedi, F. G. S. Toledo, D. F. Markgraf, D. H. Pesta, L. Mastrototaro, E. de Filippo, C. Herder, M. Jähnert, J. Weiss, K. Strassburger,

M. Schlensak, A. Schürmann, M. Roden, Dynamic changes of muscle insulin sensitivity after metabolic surgery. *Nat. Commun.* **10**, 4179 (2019).
67. S. Kahl, S. Gancheva, K. Straßburger, C. Herder, J. Machann, H. Katsuyama, S. Kabisch, E. Henkel, S. Kopf, M. Lagerpusch, K. Kantartzis, Y. Kupriyanova, D. Markgraf, T. van Gemert, B. Knebel, M. F. Wolkersdorfer, O. Kuss, J.-H. Hwang, S. R. Bornstein, C. Kasperk, N. Stefan, A. Pfeiffer, A. L. Birkenfeld, M. Roden, Empagliflozin effectively lowers liver fat content in well-controlled type 2 diabetes: A randomized, double-blind, phase 4, placebo-controlled trial. *Diabetes Care* **43**, 298–305 (2020).
68. R. S. Livingstone, P. Begovatz, S. Kahl, B. Nowotny, K. Straßburger, G. Giani, J. Bunke, M. Roden, J. H. Hwang, Initial clinical application of modified Dixon with flexible echo times: Hepatic and pancreatic fat assessments in comparison with ^{1}H MRS. *MAGMA* **27**, 397–405 (2014).
69. J. Machann, C. Thamer, N. Stefan, N. F. Schwenzer, K. Kantartzis, H. U. Häring, C. D. Claussen, A. Fritsche, F. Schick, Follow-up whole-body assessment of adipose tissue compartments during a lifestyle intervention in a large cohort at increased risk for type 2 diabetes. *Radiology* **257**, 353–363 (2010).
70. E. Phielix, T. Jelenik, P. Nowotny, J. Szendroedi, M. Roden, Reduction of non-esterified fatty acids improves insulin sensitivity and lowers oxidative stress, but fails to restore oxidative capacity in type 2 diabetes: A randomised clinical trial. *Diabetologia* **57**, 572–581 (2014).
71. O. W. Griffith, Determination of glutathione and glutathione disulfide using glutathione reductase and 2-vinylpyridine. *Anal. Biochem.* **106**, 207–212 (1980).
72. I. Morgunov, P. A. Srere, Interaction between citrate synthase and malate dehydrogenase. Substrate channeling of oxaloacetate. *J. Biol. Chem.* **273**, 29540–29544 (1998).
73. T. Mahmood, P. C. Yang, Western blot: Technique, theory, and trouble shooting. *N. Am. J. Med. Sci.* **4**, 429–434 (2012).
74. D. Dietze, M. Koenen, K. Rohrig, H. Horikoshi, H. Hauner, J. Eckel, Impairment of insulin signaling in human skeletal muscle cells by co-culture with human adipocytes. *Diabetes* **51**, 2369–2376 (2002).
75. S. Lambernd, A. Taube, A. Schober, B. Platzbecker, S. W. Görgens, R. Schlich, K. Jeruschke, J. Weiss, K. Eckardt, J. Eckel, Contractile activity of human skeletal muscle cells prevents insulin resistance by inhibiting pro-inflammatory signalling pathways. *Diabetologia* **55**, 1128–1139 (2012).
76. S. Hartwig, E. de Filippo, S. Göddeke, B. Knebel, J. Kotzka, H. al-Hasani, M. Roden, S. Lehr, H. Sell, Exosomal proteins constitute an essential part of the human adipose tissue secretome. *Biochim. Biophys. Acta Proteins Proteom.* **1867**, 140172 (2019).
77. R. J. Lobb, M. Becker, S. Wen Wen, C. S. F. Wong, A. P. Wiegmans, A. Leimgruber, A. Möller, Optimized exosome isolation protocol for cell culture supernatant and human plasma. *J. Extracell. Vesicles* **4**, 27031 (2015).
78. R. Bruderer, O. M. Bernhardt, T. Gandhi, S. M. Miladinović, L. Y. Cheng, S. Messner, T. Ehrenberger, V. Zanotelli, Y. Butscheid, C. Escher, O. Vitek, O. Rinner, L. Reiter, Extending the limits of quantitative proteome profiling with data-independent acquisition and application to acetaminophen-treated three-dimensional liver microtissues. *Mol. Cell. Proteomics* **14**, 1400–1410 (2015).
79. J. D. Bendtsen, L. J. Jensen, N. Blom, G. Von Heijne, S. Brunak, Feature-based prediction of non-classical and leaderless protein secretion. *Protein Eng. Des. Sel.* **17**, 349–356 (2004).
80. M. Pathan, S. Keerthikumar, C. S. Ang, L. Gangoda, C. Y. J. Quek, N. A. Williamson, D. Mouradov, O. M. Sieber, R. J. Simpson, A. Salim, A. Bacic, A. F. Hill, D. A. Stroud, M. T. Ryan, J. I. Agbinya, J. M. Mariadason, A. W. Burgess, S. Mathivanan, FunRich: An open access standalone functional enrichment and interaction network analysis tool. *Proteomics* **15**, 2597–2601 (2015).
81. Y. Perez-Riverol, A. Csordas, J. Bai, M. Bernal-Llinares, S. Hewapathirana, D. J. Kundu, A. Inuganti, J. Griss, G. Mayer, M. Eisenacher, E. Pérez, J. Uszkoreit, J. Pfeuffer, T. Sachsenberg, Ş. Yılmaz, S. Tiwary, J. Cox, E. Audain, M. Walzer, A. F. Jarnuczak, T. Ternent, A. Brazma, J. A. Vizcaíno, The PRIDE database and related tools and resources in 2019: Improving support for quantification data. *Nucleic Acids Res.* **47**, D442–D450 (2019).
82. A. Gómez García, M. Rivera Rodríguez, C. Gómez Alonso, D. Y. Rodriguez Ochoa, C. Alvarez Aguilar, Myeloperoxidase is associated with insulin resistance and inflammation in overweight subjects with first-degree relatives with type 2 diabetes mellitus. *Diabetes Metab. J.* **39**, 59–65 (2015).
83. J. Liu, W. Shen, B. Zhao, Y. Wang, K. Wertz, P. Weber, P. Zhang, Targeting mitochondrial biogenesis for preventing and treating insulin resistance in diabetes and obesity: Hope from natural mitochondrial nutrients. *Adv. Drug Deliv. Rev.* **61**, 1343–1352 (2009).
84. X. Liu, H. Qu, Y. Zheng, Q. Liao, L. Zhang, X. Liao, X. Xiong, Y. Wang, R. Zhang, H. Wang, Q. Tong, Z. Liu, H. Dong, G. Yang, Z. Zhu, J. Xu, H. Zheng, Mitochondrial glycerol 3-phosphate dehydrogenase promotes skeletal muscle regeneration. *EMBO Mol. Med.* **10**, e9390 (2018).
85. D. J. Bishop, J. Botella, A. J. Genders, M. J. Lee, N. J. Saner, J. Kuang, X. Yan, C. Granata, High-intensity exercise and mitochondrial biogenesis: Current controversies and future research directions. *Physiology* **34**, 56–70 (2019).
86. M. Valapala, J. K. Vishwanatha, Lipid raft endocytosis and exosomal transport facilitate extracellular trafficking of annexin A2. *J. Biol. Chem.* **286**, 30911–30925 (2011).

Acknowledgments: We would like to thank all volunteers, A. Sutkowski, K. Tinnes, M. Esser, and A. Borchardt for excellent technical support and M. Röhling for contributing to the clinical study and training supervision. Last, we would like to pay our gratitude and our respect to our colleague H. Sell who contributed to this study and passed away in September 2019. **Funding:** This study was supported in part by the Ministry of Culture and Science of the State of North Rhine-Westfalia (MKW NRW), the German Federal Ministry of Health (BMG), and by a grant of the Federal Ministry for Research (BMBF) to the German Center for Diabetes Research (DZD e.V.), the German Research Foundation (DFG, CRC 1116/2 and GRK2576 Vivid), German Diabetes Association (DDG), and the Schmutzler-Stiftung. **Author contributions:** M.R. initiated the investigation, designed and led the clinical experiments, and wrote the manuscript. M.A. conducted clinical experiments, analyzed data, and wrote the manuscript. L.M. designed and carried out the molecular analysis and the SEV experiments and wrote the manuscript. E.d.F. and K.S.N. contributed to the SEV experiments; S.H., S.L., and H.A.-H. performed the MS experiments and analyzed the data. D.P. and T.J. performed and analyzed the respirometry data. A.S.R. conducted the TEM experiments. K.S. performed statistical analysis. S.G. and Y.K. contributed to clinical experiments. D.M. and C.H. performed laboratory analysis. K.M. and J.S. designed the study and supervised clinical experiments. All authors read, reviewed, and agreed with the manuscript content. M.R. is the guarantor of this work and hence had full access to all the data in the study and takes responsibility for the integrity of the data and the accuracy of the data analysis. **Competing interests:** The authors declare that they have no competing interests. **Data and materials availability:** All data needed to evaluate the conclusions in the paper are present in the paper and/or the Supplementary Materials. Moreover, MS-based proteomic data of serum and cell-derived SEV have been deposited to the ProteomeXchange Consortium via the PRIDE (*81*) partner repository with the dataset identifiers PXD020278 and PXD020330.

Submitted 12 April 2021
Accepted 17 August 2021
Published 8 October 2021
10.1126/sciadv.abi9551

Citation: M. Apostolopoulou, L. Mastrototaro, S. Hartwig, D. Pesta, K. Straßburger, E. de Filippo, T. Jelenik, Y. Karusheva, S. Gancheva, D. Markgraf, C. Herder, K. S. Nair, A. S. Reichert, S. Lehr, K. Müssig, H. Al-Hasani, J. Szendroedi, M. Roden, Metabolic responsiveness to training depends on insulin sensitivity and protein content of exosomes in insulin-resistant males. *Sci. Adv.* **7**, eabi9551 (2021).

ScienceAdvances

Metabolic responsiveness to training depends on insulin sensitivity and protein content of exosomes in insulin-resistant males

Maria ApostolopoulouLucia MastrototaroSonja HartwigDominik PestaKlaus StraßburgerElisabetta de FilippoTomas JelenikYanislava KarushevaSofiya GanchevaDaniel MarkgrafChristian HerderK. Sreekumaran NairAndreas S. ReichertStefan LehrKarsten MüssigHadi Al-HasaniJulia SzendroediMichael Roden

Sci. Adv., 7 (41), eabi9551. • DOI: 10.1126/sciadv.abi9551

Science Advances (ISSN) is published by the American Association for the Advancement of Science. 1200 New York Avenue NW, Washington, DC 20005. The title *Science Advances* is a registered trademark of AAAS.